Design of a Communication and Navigation Subsystem for a CubeSat Mission

by

Wolfgang Traussnig

Submitted in a partial fulfilment
of the requirements for the degree of
Master of Sciences
Of the Post-graduate University Course Space Science

Karl Franzens University of Graz
Graz, Austria

Acknowledgments

This Master Thesis has been written at the Institute of Communication Networks and Satellite Communications at Graz University of Technology in the years 2005/06.

I would like to thank my thesis advisor, Univ.-Prof. Dr. Otto Koudelka, for his support in helping me complete this Diploma Thesis. I would also like to thank Univ.-Prof. Dr. Helmut Rucker for teaching me numerous issues of space physics and providing my profound information on these topics.

Finally I'd like to thank to my parents for providing me necessary support and making this study possible.

Graz, Winter 2006/2007 Wolfgang Traussnig

Abstract

This Diploma Thesis describes a design for a communication and scintillation payload subsystem on board the student satellite ACS. This different subystems are a part of a bigger project where other participants have worked on different subsystems on board of ACS. The aim of the ACS- project has been to build a satellite which is a follow up satellite of the TUGSAT-1.

The use of a dipole antenna for the S Band frequency of 2.2 GHz and a GPS patch antenna for the scinitillation payload are recommended in this Diploma Thesis. The antennas and all mechanical components will be placed on the nadir side, the side which faces earth after stabillisation, so that all other sides on the CubeSat can be used for solar panels. The GPS system will be used first for a real-time 3-dimensional navigation system and second for a comparison of the GPS signal strength at a point at two different times. A Link Budget analysis for three different Ground Station antenna types concludes this Master Thesis.

Kurzfassung

Diese Master Thesis beschreibt ein Design für ein Kommunikations Subsystem und ein GPS Szintillations Experiment an Bord des CubeSats, ACS. Dieses Subsystem und Experiment sind ein Teil eines grösseren Projektes, an dem mehrere Projektanten an unterschiedlichen Subsystemen gearbeitet haben. Das Ziel des ACS Projektes ist es, einen Pico Satelliten zu entwickeln, der dem TUGSAT-1 Projekt folgen könnte.

Für die Kommunikation im S Band (2.2 GHz) wird eine Dipol Antenne und für das GPS Szintillations Experiment eine Patch Antenne verwendet. Die Antennen und alle mechanischen Komponenten müssen auf der Nadirseite des CubSats, die Seite die nach der Stabilisation auf die Erde blickt, angebracht werden, damit alle weiteren Seiten für Solarzellen benutzt werden können. Das GPS System wird einerseits für eine 3-dimensionale Realzeitnavigation und andererseits für das GPS Szintillations Experiment genutzt.
Nachdem ein mögliches Design des Subsystem und Szintillations Experimentes vorgestellt wurde, werden noch Berechnungen der Leistungsbilanz von drei verschiedenen Bodenstationen mit verschiedenen Datenraten vorgenommen.

Table of Contents

List of Figures

List of Tables

List of Abbreviations

ACS	Austrian CubeSat
ADC	Analog-to-Digital-Converter
AMSAT	Radio Amateur Satellite Corporation
ARS	Antenna Rotator System
ASK	Amplitude Shift Keying
BFSK	Binary Frequency-Shift Keying
BPSK	Binary Phase-Shift Keying
C/A	Coarse Acquisition
Cal Poly	California Polytechnic State University
CAC	CubeSat Acceptance Checklist
CCSDS	Consultative Committee for Space Data Systems
CMOS	Complementary Metal Oxide Semiconductor
C/No	Signal to Noise
COM	Communication
COTS	Commercial Off-The-Shelf
CW	Continuous Wave
DPSK	Differential Phase-Shift Keying
DSP	Digital Signal Processor
HDLC	High-level Data Link Control
EM	Electro Magnatic
EPS	Electrical Power System
FCC	Federal Communications Commission
FEC	Forward Error Correction
FM	Frequenz Modulation
FPGA	Field Programmable Gate Array
FSK	Frequency Shift Keying

GP	Groung Plane
GPS	Global Positioning System
GS	Ground Stadion
GSE	Ground Support Equipment
IARU	International Amateur Radio Union
HPTM	High Power Transmit Mode
LV	Launch Vehicle
LPTM	Low Power Transmit Mode
MECH	Mechanical
MPa	Mega Pascal
MTP	Mission Test Plan
NASA	National Aeronautics and Space Administration
NM	Navigation Message
OBC	On Board Computer
OSI	Open Systems Interconnection
P	Precise
PAI	Polyamidimid
PC	Personal Computer
PCB	Printed Circuit Board
P/L	Payload
POM	Polyoxymethylene
P-POD	Poly Picosatellite Orbital Deployer
PSK	Phase Shift Keying
RBF	Remove Before Flight
RF	Radio Frequency
RTTY	Radio Teletype
RX	Receive
SBAS	Satellite-Based Augmentation System
SLE	Space Link Extension
SNR	Signal-to-Noise Ratio
SoC	System on a Chip

SRD	Short Range Device
SRLL	Simple Radio Link Layer
SSB	Single Side Band
SSO	Sun-Synchronous Orbit
SSTV	Slow Scan Television
TEC	Total Electron Content
TNC	Terminal Node Controller
TX	Transmit
UTC	Co-ordinated Universal Time
VHF	Very High Frequency
VSWR	Voltage Standing Wave Ratio

1 Introduction

1.1 Small Satellites

In the past few years much of the attention of the space industry has shifted towards the development of small satellites. These satellites, often called picosats, nanosats, or microsats are generally less than 200 kg and, in many cases, are as little as 1 - 5 kg. Such satellites, which range in size from refrigerators to small soda cans, offer many potential benefits over traditional space satellites [Ssc05].

Traditional space satellites are typified by geostationary communications satellites which range in mass from 500 to 7000 kg [Ssc05]. Such satellites require millions of dollars to develop and have historically been large expensive projects requiring five to ten years to construct. Because of the enormous costs and time allocated to such projects, very little risk tolerance exists. As a result, very little room exists for innovation and such satellites are often limited to the use of space-proven, though often outdated, technologies. Furthermore, an enormous amount of money and effort is placed into the development of redundant systems and the maintenance of outdated techniques and procedures. As a result of the resources required, the development of traditional satellites has historically been limited to first world counties with large military and commercial budgets.

Small satellites provide an amazing alternative to traditional space satellites. Such projects are driven by a "smaller, faster, better, cheaper, smarter" mentality which allows for a fully functioning space satellite to be built in a fraction of the time and cost of a traditional space satellite [Ssc05]. Often, such satellites may be designed, built, and launched within a period of six to thirty-six months with labor investments of a few to ten man-years.

As a result of the inexpensive nature and short development time of small satellites, project developers are more willing to accept higher risks and an increased probability of mission failure. The designs of small satellites are more open to the use of new, unproven technologies. Often such technologies not only reduce the size, weight, and cost of the satellite, but also greatly increase the available functionality. Small satellite projects are also able to accept higher risk payloads, allowing for more interesting satellite experiments. Furthermore, as a result of resource limitations, small satellite developers are often forced to experiment with new and innovative designs, techniques, and procedures.

One of the driving philosophies of small satellite design is the use of standard, easy to use, COTS components designed for nonspace applications. This allows for fast and inexpensive construction, reducing satellite complexity. The use of standardized platforms and reusable components further shortens the development process.

The low cost and limited time investment required to construct small satellites greatly reduces the cost of entry to space. Such projects make space much more accessible to amateurs, researchers, entrepreneurial efforts, and small governments [BJ04], [LLM+02]. Over the past decade an enormous variety of small satellites have been developed including a large number of educational efforts by universities [ABV+04], [WHC05].

1.2 CubeSat Satellite

To both further speed up the development process and aid in obtainment of a launch opportunity, many university small satellite projects choose to follow the CubeSat specification. This standard outlines a set of physical launch interfaces as well as mechanical requirements for a small satellite (see Appendix A).

According to this specification, a standard CubeSat satellite is a 10 x 10 x 10 cm cube weighing at most one kilogram. Currently, up to three such cubes may be combined, creating a single satellite of dimensions 10 x 10 x 30 cm with a maximum mass of 3 kg.

Small satellite projects such as CubeSat often are troubled by a similar set of difficulties and limitations. Educational projects are often limited in terms of time, student experience, financial budget, and development infrastructure. Payloads are very limited in terms of physical space available due to the extremely restricted size and mass of a CubeSat satellite. This seriously restricts payloads requiring large optics or bulky components. The limited surface area of a CubeSat restricts the amount of solar power that may be generated, restricting power available for computation, communications, and payloads.

Restrictions on space, time, and power necessitate that CubeSat satellites incorporate limited payloads, slow communications links, little redundancy, and minimal information processing capabilities. Nevertheless, many CubeSat satellites are surprisingly complex and ambitious.

One such satellite could become the Austrian CubeSat satellite designed of participants of the post-graduate University Course Space Science.

1.3 The Design of the CubeSat Mission

This CubeSat satellite will be a one-cube satellite constructed at the Graz University of Technology over the course of few years. The primary mission of the satellite is to provide a large interdisciplinary educational project for graduate engineering students.

The ACS satellite is planed as a follow up project from the TUGSAT-1 project. The TUGSAT-1 is a nanosatellite with a mass of 5 kilograms. The development time should be 2 years in cooperation with the Universitiy of Vienna and the University of Toronto. This satellite is a part of the BRITE-Austria mission [Tug].

ACS is currently expected to be launched into a 900 km low earth orbit along with other CubeSat satellites. While built largely as an educational project for students, the ACS satellite also has a number of science and technology mission objectives.

The first scientific payload consists of two different experiments and will be developed based on the estimated power budget and the scientific requirements to be fulfilled by the satellite. One experiment may measure the impact of cosmic radiation on radiation hardened and standard FPGAs working in parallel. While the radiation hardened FPGAs will be immune to cosmic radiation, the standard FPGAs will be affected by the cosmic radiation and therefore produce errors.

The second experiment of the satellite is an on-board camera, which shall take pictures of the Earth and the sky. The pictures shall be pre-processed (encoded) with the FPGAs using different encoding algorithms, and then transmitted to the ground station using the CCSDS telemetry scheme and standard radio frequencies used by CCSDS, allowing the data to be received by numerous ground stations [Pol05].
Third, ACS will attempt to demonstrate the use of an active attitude control system. Magnetic torque coils will generate magnetic fields which will interact with the Earth's field, creating the necessary torque to orient the satellite into favorable positions. Feedback on satellite orientation will be provided by a collection of sensors. The successful demonstration of active attitude control onboard a CubeSat satellite will be critical in establishing small satellites as a viable platform for payloads requiring a high degree of control of satellite orientation. This orientation will be nessesarey for the real-time 3-dimensional navigation and a potential GPS scintillation experiment.

Finaly, communication with a ground station on Earth is made possible through the use of a 2.2 GHz communication subsystem. After discussion of a possible design of ACS, calculations regarding the link budget for the uplink and downlink are carried out in this Thesis. These calculations are necessary to guarantee reliable communication between a ground station and the satellite.

This thesis will outline the design of a 2.2 GHz communication subsystem using the CCSDS standard. The process of designing the communication subsystem will be treated in Chapter 2. Chapter 3 will have a focus on the real-time 3-dimensional navigation and GPS scintillation payload. Finally, Chapter 4 will give Link Calculations for different Ground Station antenna types. Further technical details of the CubeSat and the Link Budget will be detailed in Appendices A and B.

2 Design of a 2.2 GHz Communication Subsystem

The structure of a CubeSat is shown in Figure 2.1.The satellite consists of several different subsystems with each their specific task.

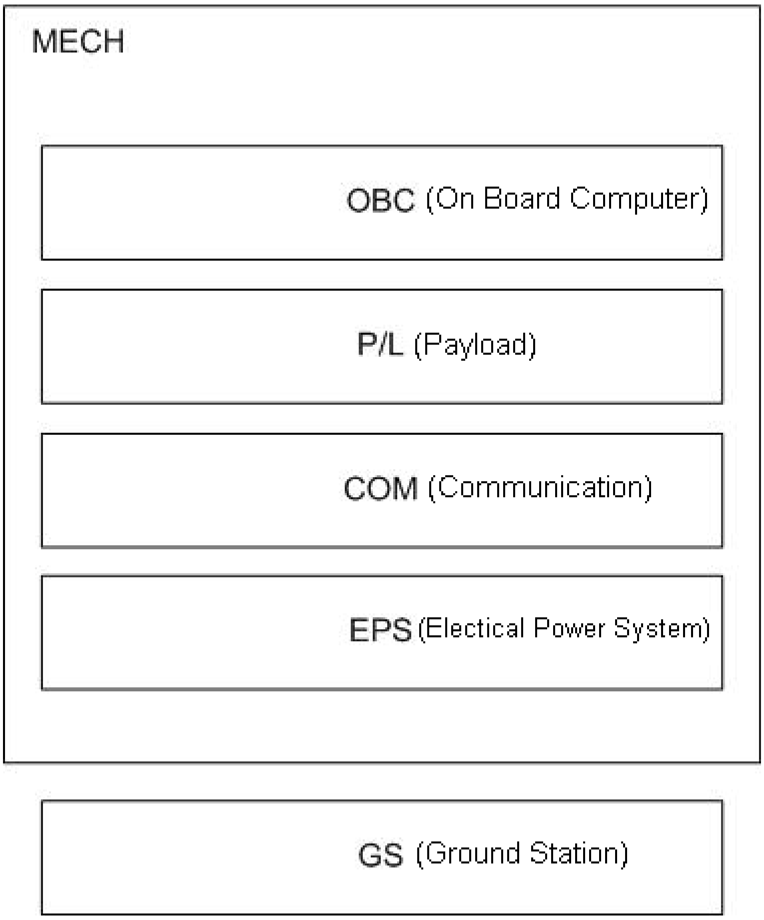

Figure 2.1: CubeSat Structure

The communication subsystem of a CubeSat (Figure 2.2) is of equal importance as that of the Ground Station. The communication subsystem aboard the CubeSat has to send various information and data down to the ground station and receive commands from the GS. There are several constraints, additional to that of the GS, which must be considered in designing the CubeSat communication subsystem.

The template of the CubeSat set the primary constraints in selection of components. The CubeSat specification restricts using any components occupying a volume greater than 10 x 10 x 10 cm. In addition, the CubeSat template also restricts using components of total mass greater than 1 kg. The structure of a CubeSat typically weights 200 to 250 g, and another 250 to 300 g should be reserved for the payload, leaving only 450 to 550 g for the power supply subsystem, storage and the electronics itself. Adding the weights there are only 120 to 170 g for the communication subsystem left.

Due to these two primary constraints, the highest priorities in the selection of components were based on physical volume and weight of each component.

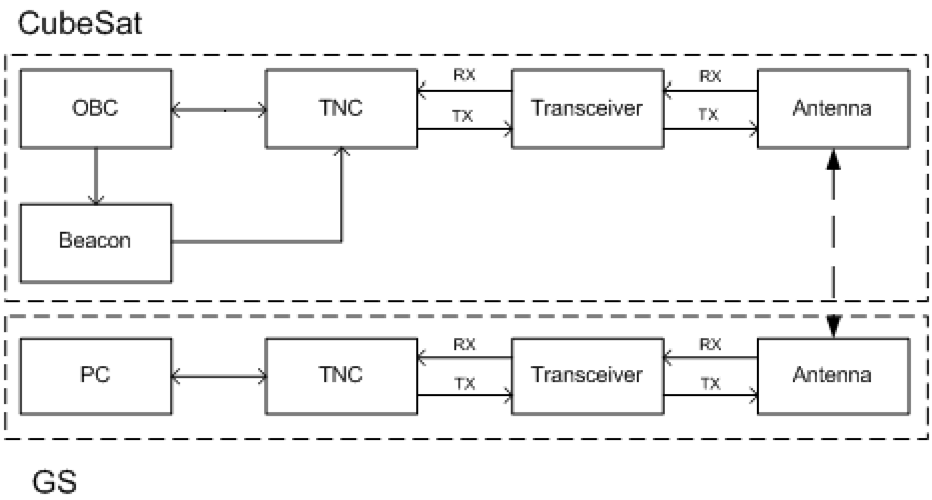

Figure 2.2: Communication Block Diagram

The final major constraint was the limited time available for design, building, testing, analysis and refinement. Because of the time constraint purchasing and modifying COTS products is favoured for the communications subsystem.

The following Chapters 2.1 and 2.2 describe briefly the amateur frequency, free licence and S Band and an example of a existing VHF/UHF communication subsystem.

2.1 Amateur Frequency, Free Licence and S Band

The AMSAT organisation is a non-profit scientific and educational corporation. It is a worldwide group of Amateur Radio Operators who share an active interest in building, launching and then communicating with each other through non-commercial Amateur Radio satellites. AMSAT groups have played a key role in significantly advancing the state of the art in space science, space education and space communications technology [Ams].

The IARU works closely with AMSAT organization: in many administration organizations, which primary goal are to co-ordinate and notify to maximize the use of the radio spectrum and to minimize interference.

2.1.1 Regulations

IARU and AMSAT has issued a paper to aid prospective owners and operators of satellite planned to operate in frequency bands allocated to the amateur satellite service. Co-operating amateur groups have drawn band-plans to help minimize interference between different operations conducted in these frequency allocations. An AMSAT organization can assist in the planning of operating, control and telemetry frequencies for best results in conjunction with other amateur satellites as well as terrestrial operators around the world. Frequency allocations for the amateur-satellite service which are shared with other services are the bands: 144 – 148 MHz, 435 – 438 MHz, 1260 – 1270 MHz, 2400 – 2450 MHz and some higher frequencies [Cla05] (see Table 2.1). Formal ITU notification is not required for the use of bands allocated to the amateur-satellite service exclusively. Even so, international notification is an advantage to the amateur-community [Itu]. AMSAT state that organizations building satellites should determine if it is possible to comply with the requirements of the amateur-satellite service or if licensing and operation should be in same other radio service which is more consistent with the nature of the mission.

Band	Analog Uplink [MHz]	Analog Downlink [MHz]
2 m		145.845 – 145.905
70 cm	436.050 – 436.150	1260-1270MHz
23 cm (1)	1268.600 – 1268.750	
23 cm (2)	1260.100 – 1260.250	
13 cm (1)		2400.275 – 2400.425
13 cm (2)	2450 +/- 50 kHz	
6 cm	5668.600 +/- 25 kHz	
X-Band		10450 +/- 50 kHz
K-Band		24058.300 +/- 25 kHz
R-Band		47088.300 +/- 25 kHz

Table 2.1: AMSAT-Phase 3E Frequencies

All stations operating in the amateur frequency bands must be controlled by licensed amateur radio operators. International communication between amateur stations in different countries must be in plain language. This requirement includes telemetry and data exchange between users. To meet the plain language requirement, technical descriptions of all emissions, codes, and formats must be made publicly available. Spare telecommand transmissions for critical spacecraft functions are generally accepted as exempt by AMSAT from the requirement to use plain language. All telecommunication (except telecommand) operating in amateur-frequencies should be open for use by amateur radio operators world-wide [San04].

2.1.2 Amateur CubeSat Frequencies

The frequency alternatives listed in Table 2.2 are listed as Exclusive Amateur Satellite Band in the official frequency scheme, and these bands are internationally allocated.

	Alternative 1	**Alternative 2**	**Alternative 3**
Uplink frequency range	144-146 MHz	435-438 MHz	435-438 MHz
Wavelength (approx)	2 m	70 cm	70 cm
Downlink frequency range	435-438 MHz	1260-1270 MHz	2400-2450 MHz
Wavelength (approx)	70 cm	24 cm	12.5 cm

Table 2.2: Amateur Frequency Alternatives for a CubeSat

The higher frequencies are suitable for downlink because they provide higher bandwidth for the data transmission. Uplink frequencies are mainly used for telecommand and handshaking, where a low data rate is sufficient. Therefore, the lower frequencies, which provide cheaper power-generation, can be used.

Other possible frequency-choices are the unlicensed 433 MHz, 868 MHz and 915 MHz SRD Band.

One major drawback of these bands which have no given protection, is the considerable noise and interference which occurs especially in urban areas. Intended applications for these frequency locations, are among others alarm and security systems, horn automation, remote control, surveillance, toys and remote keyless entry. Nevertheless, these frequencies may be used if the ground station is located in a place where interference from these short-range applications would not be a problem. The S Band covers the frequency range from 2 to 4 GHz. Most of this frequency range offers less noise and interference and can be utilized with small antennas due to the short wavelength. Most of this band requires an official license, but there are exceptions like the amateur-allocated 2.4-2.45 GHz.

The license- free bands are the easiest accessable frequency range since they do not require a formal license. The fact that anyone can use these bands, will also introduce a considerable amount of noise and interference especially from consumer-electronics. From the licensed bands we have considered, it is the requirements of the amateur-frequencies that is easiest to fullfil. It is desirable to use a high frequency to obtain more bandwidth and smaller physical antenna-size in the satellite.

An example for a communication subsystem using amateur radio band frequencies (145. 835 and 437.445 MHz) is illustrated in Chapter 2.2.

2.2 VHF/UHF Communication Subsystem

When using amateur radio band frequencies it should be noted, that the combination of uplink frequency, downlink frequency and transmission mode are all lumped togeter into standardized satellite modes [Ams]. A summary of this common satellite modes is given blow:

A This mode requires a 2 m SSB/CW transmitter and a 10 m SSB/CW receiver and supports CW and voice.

B This mode requires a 70 cm SSB/CW transmitter and a 2 m SSB/CW receiver and supports CW and voice. Some satellites also support RTTY and SSTV in this mode.

K This mode requires a 15 m *SSB/CW* transmitter and a 10 m SSB/CW receiver and supports CW and voice. This mode is unique in that it can be done with a simple HF rig.

JA This mode stands for JAnalog and requires a 2 m SSB/CW transmitter and a 70 cm SSB/CW receiver and supports CW voice.

JB This mode stands for JDigital and requires a 2 m FM transmitter and a 70 cm SSB/CW receiver and supports packet ratio data.

T This mode requires a 15 m SSB/CW transmitter and a 2 m SSB/CW receiver and supports CW and voice.

S This mode requires a 70 cm SSB/CW transmitter and a 2.4 Hz SSB/CW receiver and supports CW and voice. Many people use a 2.4 GHz to 2 m converter with a 2 m SSB/CW receiver instead of buying a 2.4 GHz SSB/CW receiver.

Some satellites have dual modes that operate simultaneously. For example, AMSAT OSCAR-13 can operate in Mode BS which means that it can do both Mode B and Mode S simultaneously. Other common dual modes are KT and KA.

The best modes are the Mode J (commonly used by AMSATs) and the Mode B (most RF efficient)

The Norwegian NCUBE satellite uses the Mode J for the VHF/UHF Communication Subsystem [Ott02]. Examples of transceivers are given below:

- Yaesu VX-1R Transceiver (Figure 2.3)
- PicoPacket TNC (Figure 2.4)

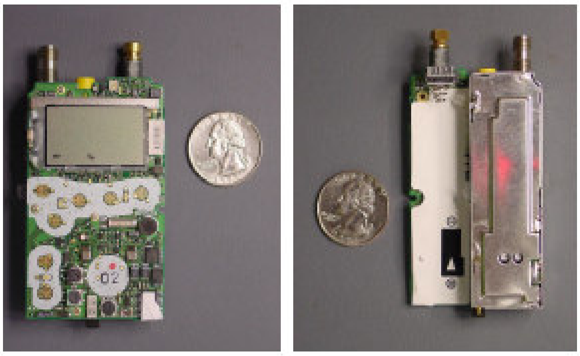

Figure 2.3: Yaesu VX Front / Bottom View

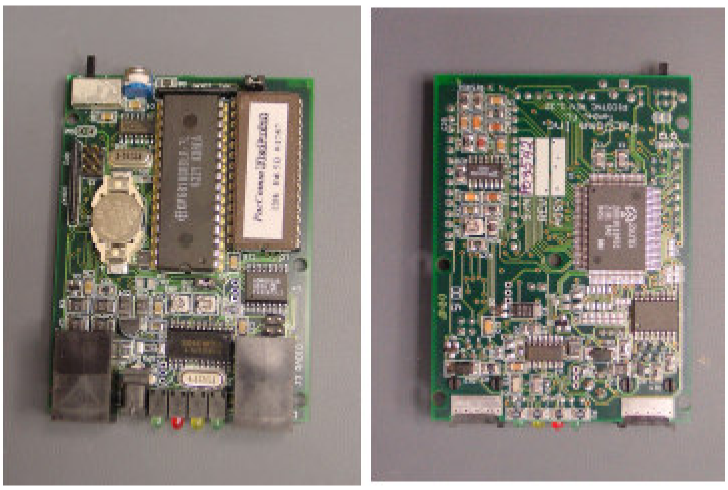

Figure 2.4: PicoPacket TNC

The VHF/UHF Communication Subsystem weighs less than 140 g and occupies a total volume (including antennas and interconnects) of 180 cm^3, less than 1/5 of the total spacecraft weight and volume budgets, with hardware cost of less than $400.

Many CubeSat communication subsystems use the AX.25 or SRLL Protocol at 1200 baud. Uplink is at a frequency of 145.835 MHz (2 m) with 20 kHz of available bandwidth. Downlink is at 437.445 MHz (70 cm) with a 30 kHz bandwidth. The communication flow is controlled by the OBC flight processor, which is linked through a 9600 baud RS232 serial connection to the TNC [Eit02].

The entire communications link (GS - CubeSat - GS) is seamless, initialized by a single encrypted uplink command. Upon contact with CubeSat, the GS instructs the processor to dump the contents of its memory into the TNC, which packetizes the binary data and keys the transmitter. The TNC consists of a single shielded PCB measuring 8.45 cm long by 6.17 cm wide, weighing 57 g. It is powered by 7-14 VDC and draws between 50 mA and 70 mA during continuous operation. The transceiver is the Yaesu VX-1R, arguably one of the smallest and lightest handhelds on the market. The radio is one double-sided PCB measuring 8.32 cm long and 4.20 cm wide, weighing only 47 g. The shielded RF module is 1.20 cm high and occupies one half of the PCB. Power is supplied from a bus for 1 W of RF output. Current consumption for the receiver and transmitter is 150 mA and 400 mA, respectively. Transmission duration for the expected 100 Kbytes/pass of telemetry and payload data at 1200 baud is about 11 minutes, comparable to the above-the-horizon window.

The CubeSat antenna is a center-fed dipole tuned to the 2 m uplink, which is nearly harmonic with the 70 cm downlink. The antenna consists of two 48 cm long Nitinol tape measure to avoid binding to the attitude control magnets. Each element is uncoiled on orbit from opposing sides of the spacecraft.

The NCUBE flight communications subsystem hardware consists of four functional blocks (Figure 2.5), the RS-232 serial interface with the OBC, the Yaesu VX-1R transceiver; the PicoPacket TNC; and the antenna assembly.

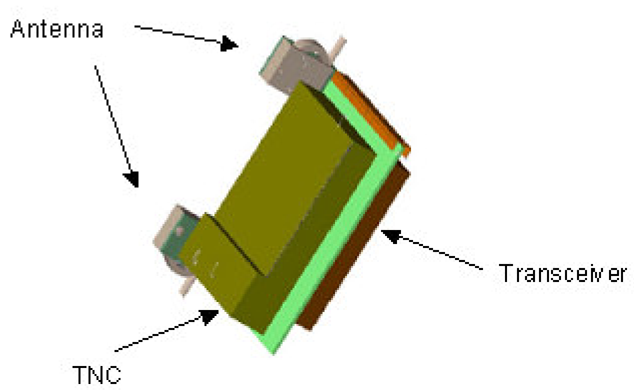

Figure 2.5: NCUBE Flight Communication Subsystem

The antenna is a center-fed dipole tuned to the 2 m uplink, which is close to harmonic with the 70 cm downlink. The antenna consists of two 48 cm Nitinol tape measures housed in opposing dielectric housings cups and connected to the transceiver using a short length of coaxial cable. The electrical connection is via the metal mounting screw used to connect the antenna cup to the subsystem PCB.

The antenna cups (Figure 2.6) are chosen for its low-friction properties. Prior to launch each element is rolled up and inserted into the cup, secured in place by a nylon fishing line. On orbit, a small resistor is heated to melt each nylon tie-down, releasing each antenna element.

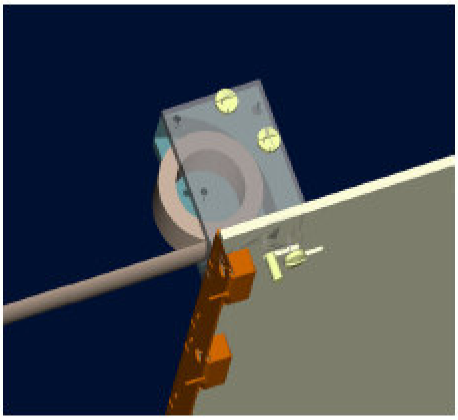

Figure 2.6: Antenna Housing and Mount

In a height of 700 to 740 km the satellite will experience a great difference in temperature. To cope with this we have to be sure that the materials in use can deal with these strict demands.

The NCUBE project group tested out two plastic types for the antenna housing boxes. One was POM (Polyoxymethylene), and the other was PAI (Polyamidimid). The POM plastic has the characteristic that it could withstand a temperature range from -40°C to +100°C for long term use and a maximum up to +140°C for shorter periods. The PAI plastics long term upper temperature is +260°C and +280°C for short term use. No lower temperature is listed for this material [Ott02a].

2.3 Antenna Design for 2.2 GHz

The antennas are essential components in a communication satellite. Their purpose is to provide a transition from a guided wave on a transmission line to a free-space wave and vice versa in the receiving case. If the antennas fail to work the satellite can be considered dead [Stu98].

The ACS is going to receive at 2.2 GHz and going to transmit at 2.2 GHz with 30 kHz bandwidth. Possibilities are a single patch antenna, or an array of patches or a helix antenna or a dipole antenna.

2.3.1 Patch Antenna

The patch antenna shown in Figure 2.7, is a type of micro strip antenna. These types of antennas are popular because of their low profile and because they easily can be fitted to different geometries. The patch antenna consists of a rectangular metal plate printed onto a dielectric substrate with ground plane on one side. The metal plate is exited directly by a micro strip line, a coaxial connection through the substrate or indirectly from a micro strip on a substrate beneath the ground plane.

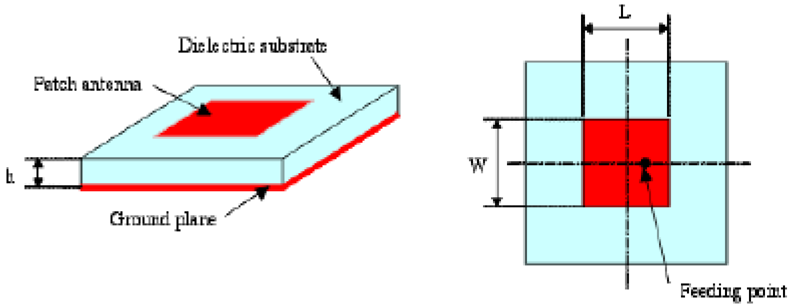

Figure 2.7:Geometry of a Micro Strip Patch Antenna

This type of antenna requires a stable satellite with the antenna facing the earth all the time. When configured as an array, a relative high gain can be achieved. No deployment is required for such an antenna. The drawback may be its limited bandwidth.

The substrate thickness is much less than a wavelength. It is most commonly operated near resonance in order to obtain real-valued input impedance. Formulas are available to estimate the resonant length, but adjustments are often necessary in practice. The physical length of the radiating patch is related to the different geometrical and electrical parameters by the following equations [Cle04]:

$$L_P = L - 2\Delta L \qquad with \qquad L = \frac{c}{2f_r\sqrt{\varepsilon_{re}}}$$

where c is the velocity of the light, f_r is the resonant frequency and ε_{re} is the effective permittivity, and

$$\Delta L = 0.412h \frac{\varepsilon_{re} + 0.3}{\varepsilon_{re} - 0.258} \frac{W/h + 0.264}{W/h + 0.813}$$

where W is the patch width, and h is the substrate thickness.

2.3.2 Helix Antenna

Helical antennas have long been popular in applications from VHF to microwaves requiring circular polarization, since they have the unique property of naturally providing circularly polarized radiation. One area that takes advantage of this property is satellite communications. Where more gain is required than can be provided by a helical antenna alone, a helical antenna can also be used as a feed for a parabolic dish for higher gains. As we shall see, the helical antenna can be an excellent feed for a dish, with the advantage of circular polarization. One limitation is that the usefulness of the circular polarization is limited since it cannot be easily reversed to the other sense, left-handed to right-handed or vice-versa [Kra77].

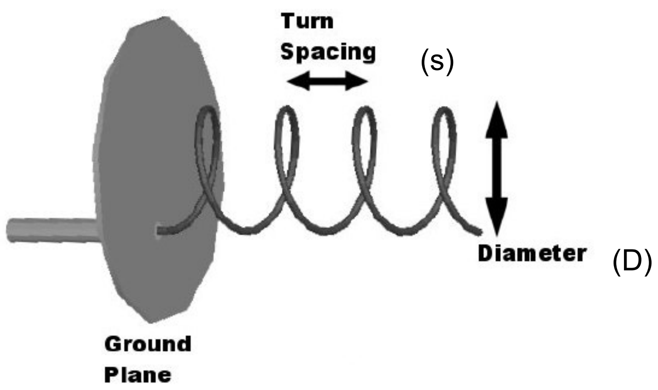

Figure 2.8: Helix Antenna

A sketch of a typical helical antenna is shown in Figure 2.8. The radiating element is a helix of wire, driven at one end and radiating along the axis of the helix. A ground plane at the driven end makes the radiation unidirectional from the far (open) end.

There are also configurations that radiate perpendicular to the axis, with an omnidirectional pattern. Typical helix dimensions for an axial-mode helical antenna have a helix circumference of one wavelength at the center frequency, with a helix pitch of 12 to 14 degrees.

The pitch angle α is defined as:

$$\alpha = \tan^{-1} \frac{s}{\pi D}$$

where s is the spacing from turn to turn and D is the diameter, the circumference divided by π. The triangle below illustrates the relationships between the circumference, diameter, pitch, turn spacing, and wire length for each turn:

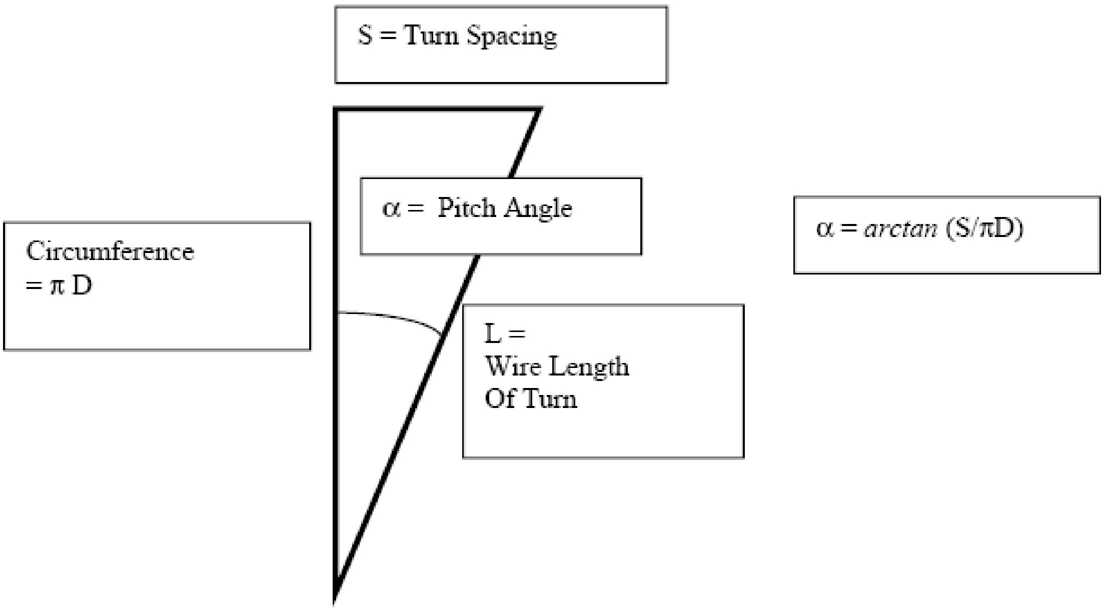

The ground plane diameter is typically 0.94λ in diameter at the center frequency, but many other configurations have been used, including square plates, wire grids, cavities, and loops. The 3 dB beamwidth for a helix with n turns is approximately:

$$BW_{3dB} = \frac{52}{C_\lambda \sqrt{n \cdot s_\lambda}} \text{ degrees,}$$

where the circumference, C_λ, and the turn spacing, s_λ, are in wavelengths. The gain of the helical antenna is also proportional to the number of turns. For higher gains, arrays of multiple helixes are needed, or other types of antennas.

Some of the AMSAT satellites and others require more than 15 dB gain with circular polarization for good reception. Until someone finds an optimization that yields higher gain from a long helix, some other antenna type is needed; a parabolic dish is often a good choice for the ground station. While a large dish can provide of more sharp 30 dB at S Band, a small dish can easily provide the 20 to 25 dB gain needed for many satellite applications. The beamwidth of a small dish is wider than the beam of a large dish, making tracking less difficult. Of course, the dish needs a feed antenna, and a short helix is a good choice for circular polarization [Eme95].

Helical antennas are relatively broadband, typically useful over a range of frequencies relative to the helix circumference of 3/4 λ to 4/3λ, or roughly a 60% bandwidth. Most of the microwave amateur bands are spaced by about this much, so there might be the possibility of covering two bands with one helical antenna, one band at the lower limit of the antenna bandwidth and the other at the upper limit. However, we shall see that for a feed antenna, the radiation patterns are much more useful near the center of the range. Thus, the main advantage of the broadband characteristic of the helical antenna is that the dimensions are not critical.

Helical Antenna for 2.2 GHz

For a frequency of 2.2 GHz a Helix with 4 turns, 12.5 deg, 0.94λ ground plane is needed. The calculated efficiency remains high from 2.0 to 2.6 GHz, about a 25% bandwidth. At the ends of the range, the efficiency falls off and the patterns deteriorate, with higher side lobe levels, particularly at the higher-frequency end. Best f/D also varies with frequency. Figure 2.9 is a graph of efficiency and best f/D vs. frequency. Phase center is also plotted - it is reasonably constant over the lower half of the frequency range, but moves rapidly at the higher end of the range. We can conclude that this helical feed would work well on a single band, but would not provide good performance on any two adjacent amateur bands.

The ground plane size is 118 mm, or 0.94λ diameter at the center frequency. Varying this diameter by ±20%, so that the diameter is 0.94λ at the highest or lowest frequency, had little effect, as shown in Figure 2.10.

Reducing the diameter to 0.5λ lowered the efficiency slightly, while a cavity ground plane 0.94λ in diameter and λ/4 deep increased it slightly. The phase center and optimum *f*/D show only small variations near the center frequency. The only significant difference was found when the ground plane is replaced by a loop 1λ in circumference, with a second loop behind it. The loop still provides high efficiency near the center frequency, but the bandwidth is much narrower, ~20% [Kra95].

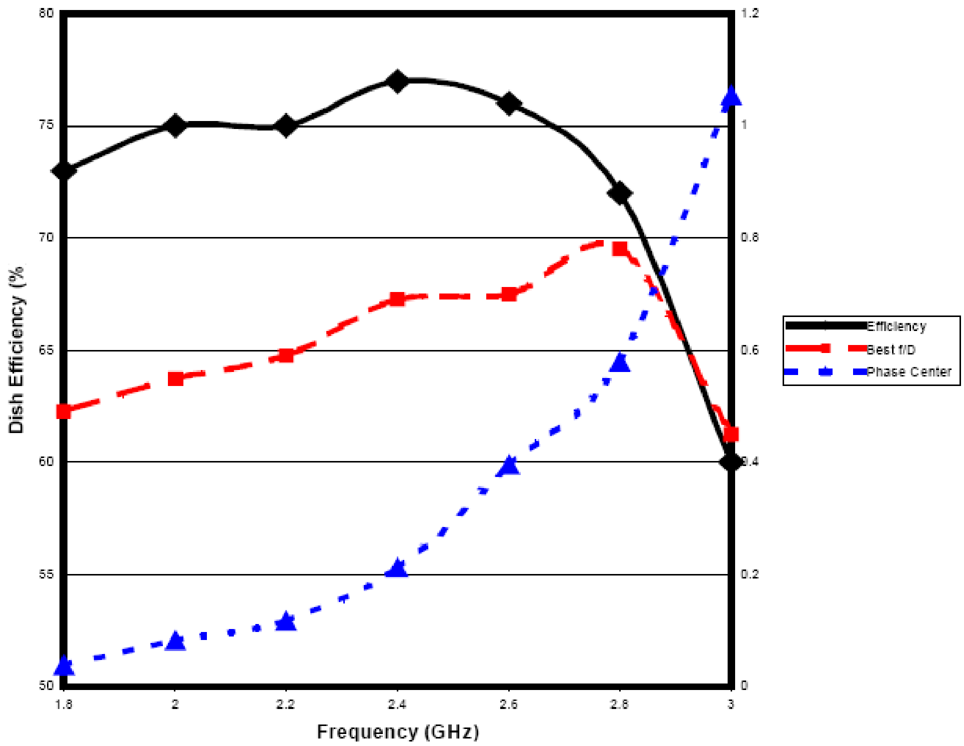

Figure 2.9: Helix feed - 4 turns, 12.5 deg, 0.94 λ Ground Plane

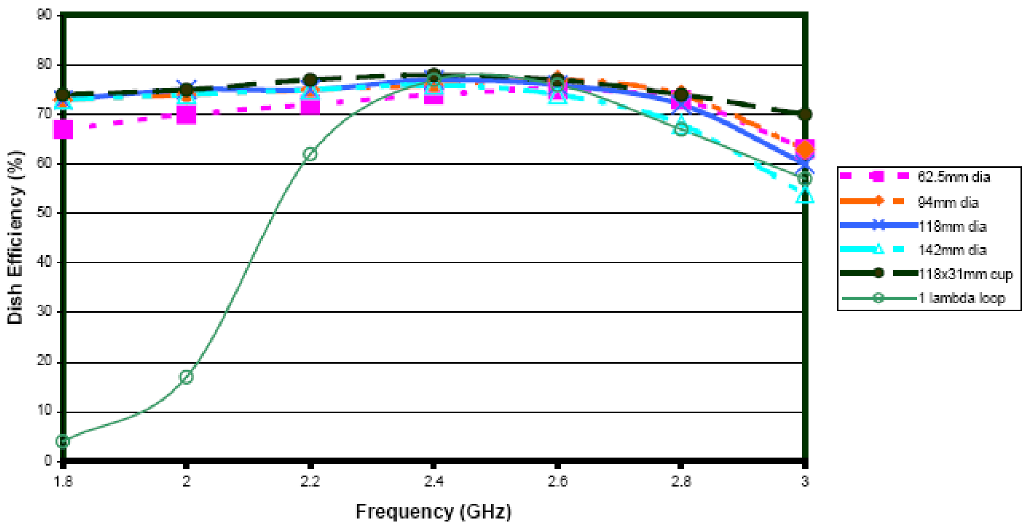

Figure 2.10: Helix feed (4 t 12.5 deg) with varying Ground Plane

2.3.3 Incremental Antenna

A incremental antenna is a straight electrical conductor connected at the center to a RF feed line. This antenna is one of the simplest and most common antennas. The dipole is inherently a balanced antenna, because it is bilaterally symmetrical. It is omni directional.

Hertzian Dipole Antenna

The Hertzian dipole is shown in Figure 2.11 and corresponds to a short length of straight wire (of length $dl \ll \lambda$ were λ is the wavelength of the sinusoidal signal) driven by an AC current of frequency ω. The wire is shown as open-ended (i.e., without termination resistances or the usual return path), with the current leading to charge increasing and decreasing at the two ends of the wire. The wire is taken as along the *z*-axis in a rectangular coordinate system.

The current *I*(*t*) is taken as a single frequency sine wave, i.e., $I_o(t) = \cos(\omega t)$. Signals

corresponding to multifrequency signals (e.g., a pass band signal as might appear in a true mobile radio system) can be considered to be composed of several sinusoids through use of the Fourier transform. However, we shall see that the radiation pattern of a linear antenna is not uniformly omnidirectional, with the directionality depending on the wavelength. [Tew05].

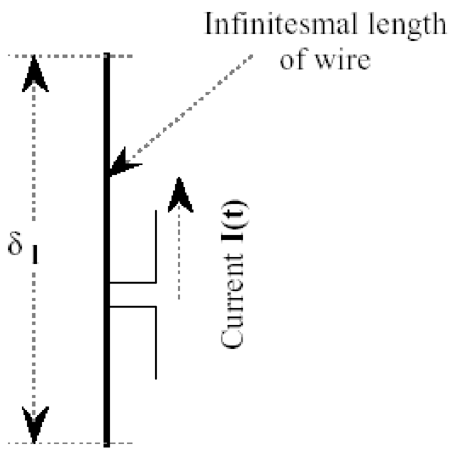

Figure 2.11: Hertzian Dipol

Electrical and Magnetic Fields, Maxwell's Equations

The electrical field $\vec{E}$ (volts/m) and the magnetic field or flux density $\vec{B}$ (Wb/m2) are vectors and the basics for an Hetzian Dipole. The following equations will give a short outline whow to calculate an Hertzian Dipole. For more informations see [Sim93].

$$\begin{aligned}\vec{D} &= \varepsilon_r \varepsilon_o \vec{E} + \vec{P} \\ \vec{D}(free - space) &= \varepsilon_o \vec{E}\end{aligned} \tag{1.1}$$

where $\vec{D}$ in free space results from $\varepsilon_r \equiv 1$ in free space. The magnetic field intensity $\vec{H}$ is related to the relative permeability μ_o and the magnetic polarization $\vec{M}$ by

$$\vec{H} = \frac{\vec{B}}{\mu_o} - \vec{M} \ . \tag{1.2}$$

Maxwell's Equations relate the electric and magnetic fields as follows:

$$\begin{aligned}\vec{\nabla} \times \vec{E} &= -\frac{\partial \vec{B}}{\partial t} \\ \vec{\nabla} \times \vec{H} &= \vec{J} + \frac{\partial \vec{D}}{\partial t}\end{aligned} \tag{1.3}$$

$$\begin{aligned}\vec{\nabla} \cdot \vec{D} &= \rho \\ \vec{\nabla} \cdot \vec{B} &= 0\end{aligned} \tag{1.4}$$

The gradient of the curl of a vector necessarily vanishes, i.e., $\vec{\nabla} \cdot (\vec{\nabla} \times \vec{A}) \equiv 0$ for any vector $\vec{A}$. From (1.4), we can therefore express the magnetic field in terms of a vector as

$$\vec{B} = \vec{\nabla} \times \vec{A} \tag{1.5}$$

Using (1.5) in (1.3), we see that we can express $\vec{E}$ in terms of this vector $\vec{A}$ as

$$\vec{E} = -\vec{\nabla} \phi - \frac{\partial \vec{A}}{\partial t} \tag{1.6}$$

where the electric scalar potential ϕ is introduced since the curl of the divergence of any scalar vanishes. This vector $\vec{A}$ is called the magnetic vector potential. Equations 1.5 and 1.6 show that, if we use the magnetic vector potential $\vec{A}$, we can readily obtain the electric and magnetic fields directly while automatically satisfying Maxwell's equations.

Magnetic Vector Potential of an Hertzian Antenna

For a length of line $\vec{\delta}_l$ carrying a current I the magnetic field is given by

$$\vec{B} = \frac{\mu_o I}{4\pi} \cdot \left(\frac{\vec{\delta}_l \times \vec{i}_r}{r^2} \right) \tag{1.7}$$

where $\vec{i}_r$ is the unit vector along the line joining the current element and the point in space of interest and *r* is the distance from the current element to the point of interest. Equation 1.7 can be simplified by noting that

$$\vec{i}_r \equiv -\vec{\nabla}\frac{1}{r} \tag{1.8}$$

Using this equivalence, (1.7) becomes

$$\vec{B} = \frac{\mu_0 I}{4\pi} \cdot \vec{\delta}_l \times \left(-\vec{\nabla}\frac{1}{r} \right) \tag{1.9}$$

$$\vec{\nabla} \times \vec{\nabla} S = S\vec{\nabla} \times \vec{\nabla} - \vec{\nabla} \times S\vec{\nabla} \tag{1.10}$$

allowing (1.9) to be written as

$$\vec{B} = \frac{\mu_0 I}{4\pi r}\vec{\nabla} \times \vec{\delta}_l + \vec{\nabla} \times \frac{\mu_0 I \vec{\delta}_l}{4\pi r} \tag{1.11}$$

which, since $\vec{\delta}_l$ is constant, becomes

$$\vec{B} = \vec{\nabla} \times \frac{\mu_0 I \vec{\delta}_l}{4\pi r} \tag{1.12}$$

Comparing (1.12) with (1.5), the magnetic vector potential due to the current elements is

$$\vec{A} = \frac{\mu_0 I \vec{\delta}_l}{4\pi r} = \left(\frac{\mu_0 I \delta_l}{4\pi r} \right) \vec{i}_z \tag{1.13}$$

where $\vec{i}_z$ is the unit vector in the *z*-direction (i.e., along the wire).

Magnetic Vector Potential for Sinusoidal Current

The current I in (1.13) was assumed at the start to be a time-varying current given by $I(t, r = 0) = I_0 \cos(\omega t)$ at the dipole. At distances away from the dipole, there is a retardation effect due to the time required for the electromagnetic field to propagate to the point $r \neq 0$, i.e., the time varying part becomes $\cos(\omega\{t - r/c)\ \} = \cos(\omega t - \beta r)$ where *c* is the propagation velocity (speed of light assuming free space propagation) of the electromagnetic signal and the phase constant $\beta = \omega / c$.

Therefore, $\vec{A} = \left(\frac{\mu_0 I_0 \delta_l}{4\pi r} \right) \cos(\omega t - \beta r) \vec{i}_z$ (1.14)

The relationship between the unit vector $\vec{i}_z$ in a rectangular coordinate system and the unit vectors $(\vec{i}_r, \vec{i}_0 \; and \; \vec{i}_\Phi)$ in a spherical coordinate system is:

$$\vec{i}_z = \cos(\theta) \cdot \vec{i}_r - \sin(\theta) \cdot \vec{i}_\theta \tag{1.15}$$

Using (1.15) in (1.14) gives

$$\vec{A} = \left(\frac{\mu_0 I_0 \delta_l}{4\pi r} \right) \cos(\omega t - \beta r)(\cos(\theta) \cdot \vec{i}_r - \sin(\theta) \cdot \vec{i}_\theta \tag{1.16}$$

$$= A_r \cdot \vec{i}_r + A_\theta \cdot \vec{i}_\theta \tag{1.17}$$

where the two components of $\vec{A}$ are given by (compare equations 1.16 and 1.17)

$$A_r = \left(\frac{\mu_0 I_0 \delta_l}{4\pi r} \right) \cos(\omega t - \beta r) \cos(\theta) \tag{1.18}$$

$$A_\Theta = -\left(\frac{\mu_0 I_0 \delta_l}{4\pi r} \right) \cos(\omega t - \beta r) \sin(\theta) \tag{1.19}$$

Electrical and Magnetical Fields for an Hertzian Dipole

$$\begin{aligned} \vec{\nabla} \times \vec{A} = & \frac{1}{r \sin(\theta)} \left[\frac{\partial}{\partial \theta} (A_\phi \sin(\theta)) - \frac{\partial A_\theta}{\partial \Phi} \right] \vec{i}_r + \frac{1}{r} \left[\frac{1}{\sin(\theta)} \frac{\partial A_r}{\partial \Phi} - \frac{\partial}{\partial r} (r A_\phi) \right] \vec{i}_\theta \\ & + \frac{1}{r} \left[\frac{\partial}{\partial r} (r A_\theta) - \frac{\partial A_r}{\partial \theta} \right] \vec{i}_\phi \end{aligned} \tag{1.20}$$

Using (1.20), $\vec{B}$ and $\vec{H}$ are given by

$$\begin{aligned} \vec{H} &= \frac{\vec{B}}{\mu_0} = \frac{1}{\mu_0} \vec{\nabla} \times \vec{A} = \frac{1}{\mu_0 r} \left[\frac{\partial}{\partial r} (r A_\theta) - \frac{\partial A_r}{\partial \theta} \right] \cdot \vec{i}_\phi \\ &= \frac{I_0 \delta_l \sin(\theta)}{4\pi} \left[\frac{\cos(\omega t - \beta r)}{r^2} - \frac{\beta \sin(\omega t - \beta r)}{r} \right] \vec{i}_\phi \\ & or \\ H_\phi &= \frac{1}{\mu_0 r} \left[\frac{\partial}{\partial r} (r A_\theta) - \frac{\partial A_r}{\partial \theta} \right] = \frac{I_0 \delta_l \sin(\theta)}{4\pi} \left[\frac{\cos(\omega t - \beta r)}{r^2} - \frac{\beta \sin(\omega t - \beta r)}{r} \right] \end{aligned} \tag{1.21}$$

Given $\vec{H}$, the Maxwell's Equationscan be used, to obtain the electric field (with $\vec{J} = 0$ at the point away from the Hertzian dipole where we are observing the fields).

Therefore

$$\begin{aligned}\frac{\partial \vec{E}}{\partial t} &= \frac{1}{\varepsilon_0}\vec{\nabla}\times\vec{H} \\ &= \frac{1}{\varepsilon_0 r^2 \sin(\theta)}\frac{\partial}{\partial\theta}(r\sin(\theta)H_\phi)\vec{i}_r - \frac{1}{\varepsilon_0 r\ \sin(\theta)}\frac{\partial}{\partial r}(r\sin(\theta)H_\phi)\vec{i}_\theta\end{aligned}$$

Taking the derivatives of H_ϕ and integrating over time yields

$$\begin{aligned}\vec{E} &= \frac{2I_0\delta_l\cos(\theta)}{4\pi\varepsilon_0\omega}\left[\frac{\sin(\omega t-\beta r)}{r^3}+\frac{\beta\cos(\omega t-\beta r)}{r^2}\right]\vec{i}_r \\ &+\frac{I_0\delta_l\sin(\theta)}{4\pi\varepsilon_0\omega}\left[\frac{\sin(\omega t-\beta r)}{r^3}+\frac{\beta\cos(\omega t-\beta r)}{r^2}-\frac{\beta^2\sin(\omega t-\beta r)}{r}\right]\vec{i}_\theta\end{aligned} \tag{1.22}$$

Equations 1.21 and 1.22 include terms close to the antenna (i.e., the so called “near-field terms"). As we move away from the dipole antenna, the terms involving r^{-2} and r^{-3} become negligible relative to the terms involving r^{-1} and can be ignored (in the “far-field region"). In fact, the distance r at which these “lower order terms" can be neglected is defined by $\frac{\beta}{r} \gg \frac{1}{r^2}\ or\ r \gg \frac{1}{\beta}$. We can relate all this to the wavelength λ.

Recall that β was defined as $\beta = \frac{\omega}{c}$. The wavelength, on the other hand, is defined as $\lambda = \frac{c}{f}$. Since $\omega = 2\pi f$, $\frac{\beta}{(2\pi)} = \frac{f}{c}\ or\ \frac{2\pi}{\lambda} = \beta$. Therefore, the far field region corresponds to $r \gg \frac{\lambda}{2\pi}$, where the fields are given by

$$\vec{H}(r \gg \frac{\lambda}{2\pi}) = -\left[\frac{I_0\delta_l\beta}{4\pi}\right]\left[\frac{\sin(\theta)}{r}\right]\sin(\omega t-\beta r)\vec{i}_\phi \tag{1.23}$$

and

$$\begin{aligned}\vec{E}(r \gg \frac{\lambda}{2}) &= -\left[\frac{I_0\delta_l\beta^2}{4\pi\varepsilon_0\omega}\right]\left[\frac{\sin(\theta)}{r}\right]\sin(\omega t-\beta r)\vec{i}_\theta \\ &= -\left[\frac{\eta I_0\delta_l\beta}{4\pi}\right]\left[\frac{\sin(\theta)}{r}\right]\sin(\omega t-\beta r)\vec{i}_\theta\end{aligned} \tag{1.24}$$

where

$$\eta \equiv \frac{\beta}{(\varepsilon_0\omega)} \tag{1.25}$$

Radiated Power and Radiation Resistance for an Hertzian Dipole

The radiation power at some point in the far field region is given by the Poynting vector $(\vec{P})$, i.e.,

$$\begin{aligned}\vec{P} &= \vec{E}\times\vec{H} \\ &= E_\theta \vec{i}_\theta \times \vec{H}_\phi \vec{i}_\phi \\ &= \left[\frac{\eta\beta^2 I_0^2 (\delta_l)^2 \sin^2(\theta)}{16\pi^2 r^2}\right]\sin^2(\omega t-\beta r)\vec{i}_r\end{aligned} \tag{1.26}$$

The total radiated power P_{rad} is obtained by integrating $\vec{P}$ over the surface of a sphere with radius *r*, i.e.,

$$\begin{aligned}P_{rad} &= \int_{\theta=0}^{\pi}\int_{\phi=0}^{2\pi}\left[\vec{P}\cdot\vec{i}_r\right]r^2\sin(\theta)d\theta d\phi \\ &= \frac{\eta\beta^2 I_0^2(\delta_l)^2}{6\pi}\sin^2(\omega t-\beta r)\end{aligned} \tag{1.27}$$

$$= \frac{2\pi\eta I_0^2}{3}\left(\frac{\delta_l}{\lambda}\right)\sin^2(\omega t-\beta r) \tag{1.28}$$

Since the average value of $\sin^2(\omega t-\beta r)=\frac{1}{2}$, the time averaged, radiated power is

$$\begin{aligned}\langle P_{rad}\rangle &= \frac{\pi\eta I_0^2}{3}\left(\frac{\delta_l}{\lambda}\right)^2\langle\sin^2(\omega t-\beta r\rangle \\ &= \frac{I_0^2}{2}\left[\frac{2\pi\eta}{3}\left(\frac{\delta_l}{\lambda}\right)^2\right]\end{aligned} \tag{1.29}$$

The term in (1.29) defines the radiation resistance (R_{rad}), defined as the value of a resistor driven by the current in the dipole antenna which would lead to the same average power dissipation as the average radiated power. Therefore,

$$R_{rad} = \frac{2\pi\eta}{3}\left(\frac{\delta_l}{\lambda}\right)^2 \tag{1.30}$$

The term η above is called the *impedance of free space* and has a standard value Impedance of free space = η = 120π Ohms.

2.3.4 Half- Wavelength Dipole Antenna

The basic structure of a dipole antenna (see Figure 2.12) is two wires, one extending in the +*z* direction and the other extending in the -*z* direction, with the sum of the lengths of these two sections being $L = \lambda/2$.

Current $I(t, z=0) = I_0 \cos(\omega t)$ is fed into the center (i.e., at the two endpoints at *z* = *0*). The current *I(t; z)* vanishes at each wire's end (i.e., at $z = \pm L$). The current at any point on the antenna is given by

$$I(t,z) = I_o \cos(\pi z / L)\cos(\omega t) \quad (1.34)$$

where $\cos \pi z / L$ represents the peak current at any point *z* along the wire.

To determine the fields well away from the antenna, each point on the wire can be viewed as a point source (Hertzian dipole antenna) and the fields for these Hertzian dipole at some distance from the antenna, given above, can be integrated over the finite length dipole antenna. In those equations above, we replace the current term I_0 with the current $I_0 \cos(\pi z / L)$, giving the various fields a *z*-dependence. The fields far away from the antenna are then obtained by integrating the expressions for the Hertzian dipole antenna (with the substitution for I_0 above) from $z = -L/2 \; to \; z = +L/2$. The final results for the fields are summarized as follows (for frequency ω and phase constant β matched to the antenna length $L \equiv \lambda/2$).

$$E_\theta = -\left[\frac{\eta I_0}{2\pi r}\right]\left[\frac{\cos\left[\left(\pi/2\right)\cos(\theta)\right]}{\sin(\theta)}\right]\sin(\omega t - \beta r)$$

$$H_\Phi = -\left[\frac{I_0}{2\pi r}\right]\left[\frac{\cos\left[\left(\pi/2\right)\cos(\theta)\right]}{\sin(\theta)}\right]\sin(\omega t - \beta r)$$

$$\vec{P} = \vec{E} \times \vec{H}$$

$$= \left[\frac{\eta I_0^2}{4\pi^2 r^2}\right]\left[\frac{\cos^2\left[\left(\pi/2\right)\cos(\theta)\right]}{\sin^2(\theta)}\right]\sin^2(\omega t - \beta r)$$

$$P_{rad} = \left[\frac{0.609 \eta I_0^2}{\pi}\right]\sin^2(\omega t - \beta r)$$

$$\langle P_{rad} \rangle = \frac{1}{2} \cdot I_0^2 \cdot \left[\frac{0.609\eta}{\pi}\right]$$

$$R_{rad} = \frac{0.609\eta}{\pi} Ohms$$

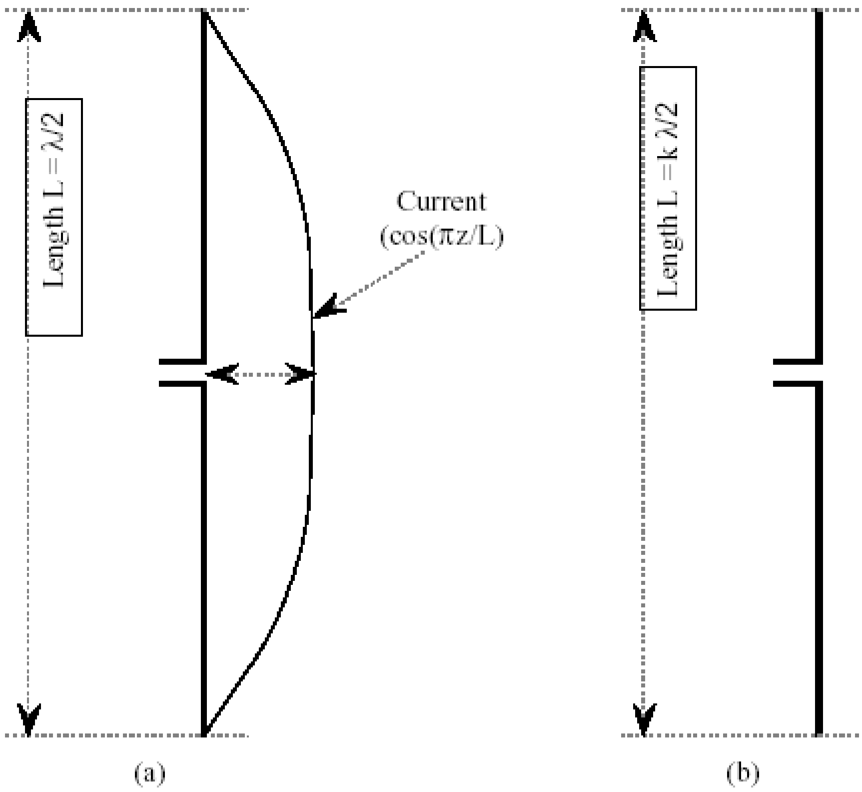

Figure 2.12: Dipole Antenna. (a) Half- Wavelength (b) Arbitrary Length Antenna

$$D = 1.642$$

2.3.5 Half-Wavelength Dipole Antenna for 2.2 GHz

A half-wave dipole antenna (see Chapter 2.3.4) is a straight electrical conductor connected at the center to a radio-frequency feed line. This antenna is one of the simplest and most common antennas. The dipole is inherently a balanced antenna, because it is bilaterally symmetrical. It is also omni directional.

Dipole antennas can be oriented horizontally, vertically, or at a slant as is the case for the S band antenna for the ACS. The polarization of the electromagnetic field radiated by a dipole transmitting antenna corresponds to the orientation of the element. When the antenna is used to receive RF signals, it is most sensitive to EM fields whose polarization is parallel to the orientation of the element. The RF current in a dipole is maximum at the center (the point where the feed line joins the element, z=0), and is zero at the ends of the element. The RF voltage is maximum at the ends and is minimum at the center.

The advantage of a half wave dipole is that it can be made to resonate and present zero input reactance.

Antenna Length (mm)	Frequency (MHz)
68.15	2200
343.2	437
1034	145

Table 2.3: Dipole Parameters

Note: For antennas in a track around the satellite the antenna impedance and the VSWR has to be simulated and calculated.

Bandwidth

Bandwidth is defined as “the range of frequencies within which the performance of the antenna, with respect to some characteristic, conforms to a specified standard”. This standard can for example be VSWR, voltage standing wave ratio, of 2.0.

Often a radio needs to work on multiple frequencies. It is however not unusual that that radio equipment have to operate in a much wider frequency band than this. This means that the antenna must perform well over a range of frequencies. So, the goal must be to make it resonant in the middle of that band.

For the dipole antenna case the general principle is that the thicker the antenna is the wider the bandwidth is (see Figure 2.13).

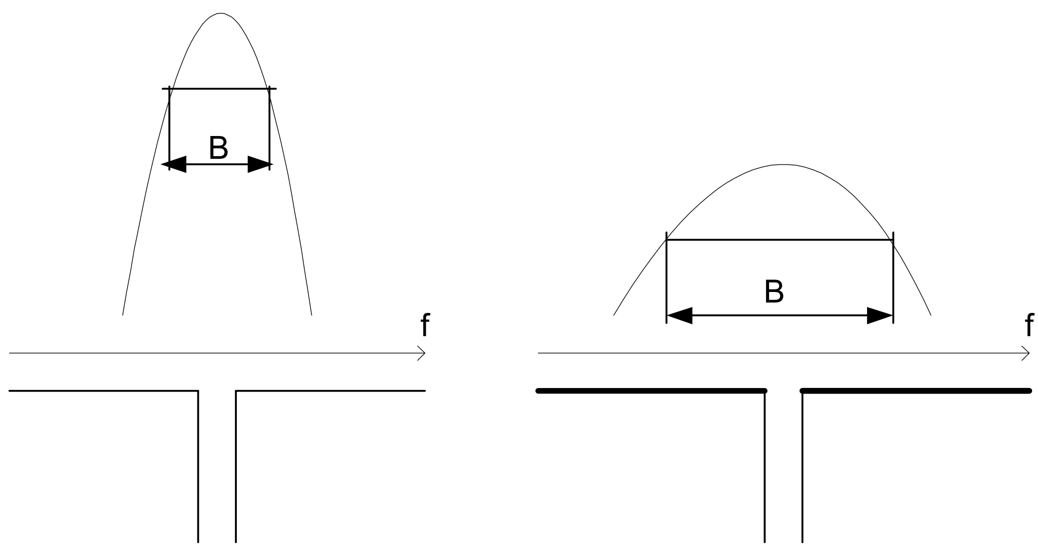

Figure 2.13: Bandwidth in Dependence of Thickness

Impedance matching

The radio communication theory says that the antenna impedance, Z_L, has to be matched to the transmission line, Z_0. The reason for this is that maximum power transfer between source and load occurs when the system impedances are matched. It also improves the signal-to noise-ratio for the system and reduces amplitude and phase errors.

The match can be described by the reflection coefficient

$$\Gamma(f) = \frac{Z_L(f) - Z_0}{Z_L(f) + Z_0}$$

and the voltage standing wave ratio

$$VSWR(f) = \frac{1 + |\Gamma(f)|}{1 - |\Gamma(f)|}.$$

The reflection coefficient varies from -1, for short load, to +1, for open load, and becomes 0 for matched impedance load.

VSWR is a measure of impedance mismatch between the transmission line and its load. The higher the VSWR is, the greater the mismatch. For a good match the voltage standing wave ratio should be under 2 for a specified frequency. When VSWR is 2.0 it is equal to 90% power absorption.

The Return Loss, S11, is also a common expression used in antenna measuring. This is basically the same thing as reflection coefficient. If 50% of the signal is absorbed by the antenna and 50% is reflected back, we say that the Return Loss is –3 dB. A very good antenna might have a value of –10 dB, 90% absorbed and 10 % reflected.

When studying a graph showing Return Loss/VSWR, a deep and wide dip of the curve is good since this shows an antenna with good bandwidth

When match in impedance is absent an impedance-matching system must be constructed, see Figure 2.14.

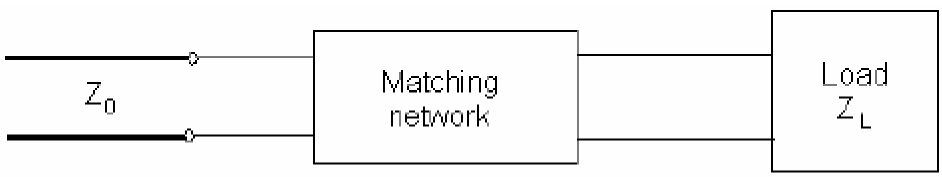

Figure 2.14: Network Matching

As long as the load impedance for the antenna, Z_L, has a nonzero real part, a matching network can always be found.

2.3.6 Antenna Deployment

When the satellite is free from the launching tube the antennas have to be folded down (CubeSat Design Specification Document, Appendix A).The antennas will be folded around the CubeSat. After the satellite is launched we have to wait a certain amount of time before we deploy the antennas. This has to be done autonomously. If deployed too early they could come in contact with the launching tube or other CubeSats.

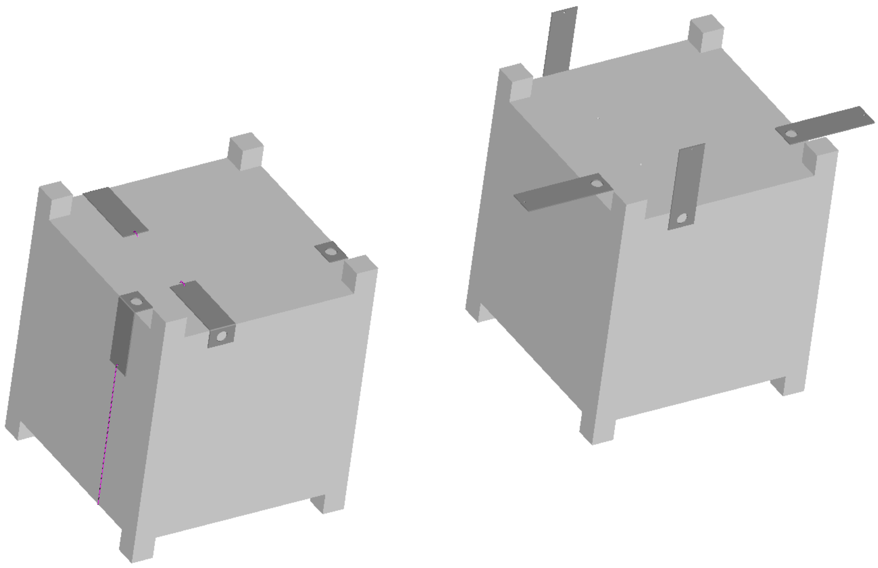

Figure 2.15: 2.2 GHz Dipole Antenna (folded and deployed)

The antennas can be deployed by using a fishing line to tie down the antennas in the track. To break the fishing line a nichrome wire can be used which will be coiled around a piece of the fishing line. This should be done at two places to make the system redundant. If one coil fails to break the wire there still is a second chance. The fishing line is broken by applying a voltage across the nichrome wire.

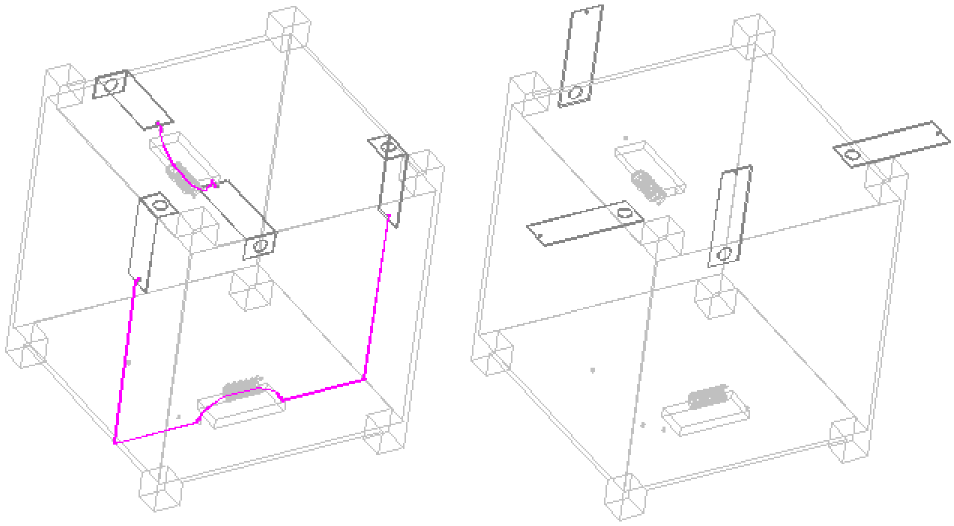

Figure 2.16: Dipole Antenna Deployment Mechanism

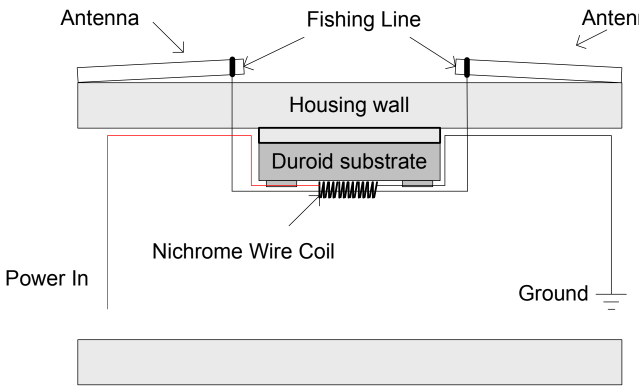

Figure 2.17: Side View of the Deployment Mechanism

Antenna Deployment Power

The antenna system will need power when deploying the antennas. The voltage level needed to break the fishing line should be somewhere between 2 and 3.5 V. This is not yet tested. An other CubeSat project has shown that the smaller we make the diameter of the nichrome wire coil and the more voltage we apply the faster the fishing line breaks. By applying 3.2 V the wire broke after 1.8 seconds. The nichrome wire coil had a diameter of 2 mm and was 3.75 mm long.

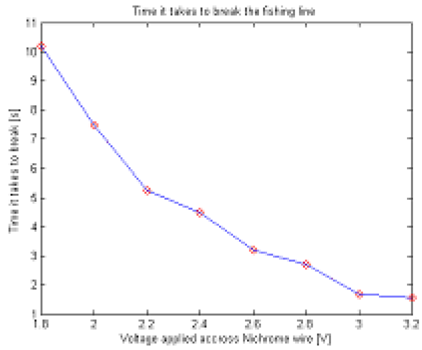

Figure 2.18: Time and Voltage to break a fishing line

Antenna Materials

When it comes to antenna materials one has to look at the different relevant properties. With regards the two main properties are conductivity and elasticity. But there are same materials that are better suited than others. Normal copper is the most used antenna material. There are unknown amounts of alloys with different characteristics. Unfortunately the problem in choosing a material is complicated. We also have to take into consideration the elasticity of the material. This property is in fact much more important than the ideal conducting material. It is necessary to find a material with good spring like capabilities. They use temperature to change their shape. Below a temperature the coils of for instance a helix antenna can be cramped together, and when the temperature rises above a certain level the metal changes its shape to erect form. However it would be rather negative to have the antenna shape changing every time the satellite went behind the earth and the temperature drops

The most likely metal to use is the standard metal-copper, Nickel-Titanium (Nitinol) or Beryllium-Copper.

Nitinol

Nitinol is a family of alloys which are comprised of near equiatomic percentages of nickel and titanium. A few variants of Nitinol also include small amounts of a third element that is used to alter certain properties. Nitinol exhibits a thermoelastic martensitic transformation. This transformation is responsible for either shape memory or superelasticity being exhibited by the alloy. Following deformation below the transformation range, the ability called shape memory allows recovery of a predetermined shape upon heating above the transformation range. Super-elasticity is the ability to recover a shape upon removal of an applied stress over a narrow range of deformation temperatures. The strain recovered with shape memory or superelasticity provides nearly ten times the elastic spring back of other alloys such as stainless steel [Smt].

Product Forms: Round wire, size range .0005” up to .250”

Flat wire, minimum thickness down to .0003”

Beryllium Copper

Beryllium copper (C17200) offers the highest tensile strength at approximately 230 KSI (1 KSI equals 6.894,757 MPa. It is used when high conductance (15-30%) and forming a rigid part or strength is needed (Resistivity 34-69 Ohm-circular, MIL/FtDensity 8.25g/cm^3 20°CDC) [Fwm].

Product Forms: Round wire, size range .001” up to .114” (230-115 KSI)

Flat wire, minimum thickness down to .0005” (230 KSI)

As shown above, both antenna materials have the same properties that will fulfill the needs for a CubeSat mission.

2.4 Disscusion

As described the ACS will have an S Band antenna for up and downlink. The S Band TX frequency is 2297.5 MHz. By using the patch antenna we need two patches on the CubeSat, one for the communication and one for the GPS payload. The micro strip (patch) is in this regard a safer antenna, but the antennas need too much space on the surface of the CubeSat. The solar cell surface ist too small for the power generation.

The helix antenna will deliver a far larger amount of data if the conditions are right. But it demands a stable satellite, and the antenna deployment mechanism do not work reliably (no redundancy is given).

The dipole antenna has been used (in a similar kind) by other CubeSat projects. And not surprisingly it has the overall best properties for a satellite with out special stability control. The only problem is the size particularly for the lower frequencies (see Chapter 2.3).

The choice of a single dipole is fourfold:

- It allows for enhanced directional gain over an omni antenna since a dipole does not require a ground plane and is not shadowed by the spacecraft
- The use of one antenna for both up-/downlink frequencies avoids the addition of duplexer hardware
- It is relatively simple to tune to both uplink and downlink frequencies
- It reduces the number of potential points of failure, and will radiate if only one element deploys.

2.5 Miniature Transceiver for 2.2 GHz

The only COTS transceiver for 2.2 GHz which fits the CubeSat Specification (see Appendix A) in weight and size is the MSX-765, developed by Telemetry-West.

The MSX-765 was designed to meet the next generation needs for command reception and telemetry transmission for military, NASA, and commercial high-reliability satellite applications where mass is critical and higher uplink command rates are required. It is compatible with DoD, NASA, and commercial TC systems [Lct05].

The MSX-765 is a DSP based design using the technologies incorporated in the CXS-2000 Flexible Architecture Secure Transponder. The unit consists of a BPSK receiver and a BPSK transmitter operating independently but physically connected for low mass. The transmitter and receiver are also available as separate units.

The receiver and transmitter exciter frequencies are synthesized from standard internal references allowing the user flexibility in frequency selection with a relatively short delivery cycle.

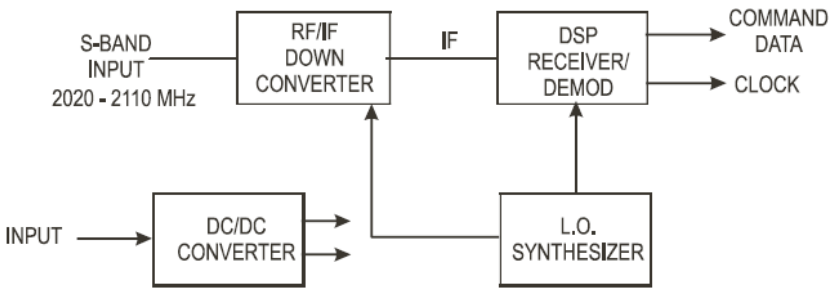

Figure 2.19: MSX-765 BPSK Receiver Block Diagram

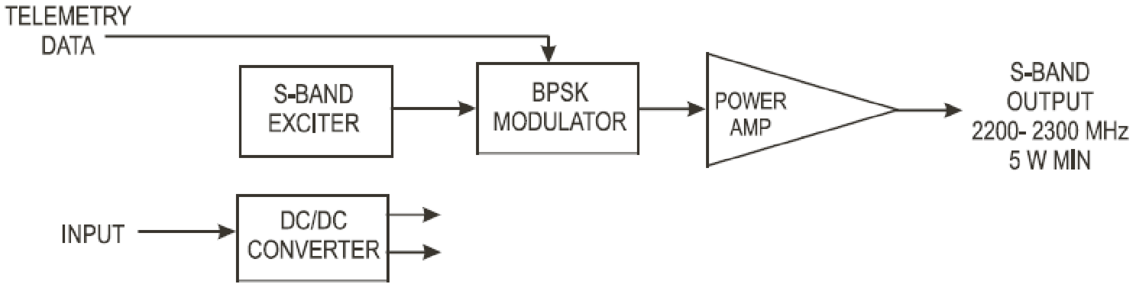

Figure 2.20: MSX-765 BPSK Transmitter Block Diagram

2.6 Transmission Protocols

The OBC must be able to communicate with the hardware on the ground station. This communication must be efficient and reliable. The satellite's communication subsystem and the communication subsystem on the ground station need same mean to decide if the data transmitted through the radios are not corrupted. To accomplish this we need same common ground rules for how the communication should take place. These rules, called protocols, will then say how the different parts of the communication subsystems should communicate to work properly.

The communication subsystem of a CubeSat has two main purposes:

- Transmit telemetry data, including a beacon.
- Provide a mean for the satellite to communicate with ground station and vice versa.

The first point is the least demanding. The communication subsystem needs only to transmit a signal with the correct data. The second point is more demanding. The subsystem should be able to receive a signal from the ground station, establish a connection, receive and send data and close the connection in a proper way.

We will here look at same possible solutions on the software part of this problem. We will limit this discussion to the data link layer, see Figure 2.21. We will not give any constraints on which layer(s) should be implemented above the data link layer. Although we will point out that what we expect the higher layer(s) to do.

The physical layer performs the task of transmitting raw bits over the communication channel. The data link layer's task is to take this stream of bits and transform it into a form that seems uninterrupted and without errors from the application layer. This is done by breaking the input data from the application layer into frames. These frames are transferred to the data link layer at the other end of the connection where the data is assembled and sent to the application layer. The data link layer checks for errors in frames and missing frames and takes appropriate actions to correct this. The data link layer looks after flow control to prevent a fast sending source from drowning a slow receiving sink.

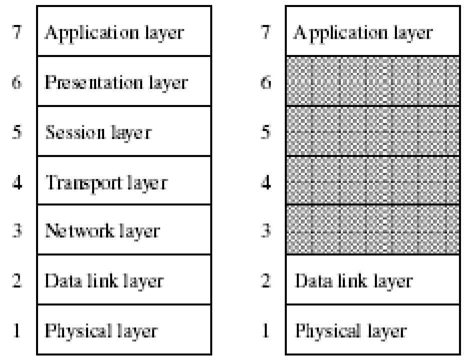

Figure 2.21: Standard OSI Model and modified Model for a CubeSat

2.6.1 AX.25 Protocol

The most used data link layer protocol between radio amateurs is AX.25, and it is also well documented. AX.25 is also implemented in most commercial TNCs. We will look at the AX.25 protocol below.

The AX.25 protocol gives an complete overview of the structure of the data link layer and the interfaces between the data link layer and the layer above and the physical layer. Same of the properties with the protocol is listed below.

Properties of AX.25 are:

- confirms to HDLC
- supports amateur call names
- supports connected links
- supports connection less links, needed for beacon
- supports half / full duplex
- supports error detection.

The structure of the lowest layers of the communication system will follow easily from the simplified OSI Model with only three layers, see Figure 2.21. AX.25 corresponds to the data link layer. The layer above the data link layer will depend how the OBC will be implemented.

AX.25 Frames

The data units of the data link layer are called frames. There are tree different types of frames:

a) Information frame (I frame)

b) Supervisory frame (S frame)

c) Unnumbered frame (U frame)

The I frames carries the data that are to be transmitted. The S frames take care of acknowledging and requests for retransmission of lost or corrupted data. The U frames are responsible for establishing and terminating link connections. With the U frames it is also possible to transmit data outside the normal flow.

The AX.25 protocol envelops the data it sends to the physical layer in a frame. The structure of such a frame is seen in Figure 2.22.

Flag	Address	Control	PID	Info	FCS	Flag
01111110	112/224 bits	8/16 bits	8 bits	N*8 bits	16 bits	01111110

Figure 2.22: Frame Construction

Limitations of AX.25

A satellite will not, as a stationary radio station, be within range all the time. In fact the satellite will only be able to communicate with the ground station for a limited duration. If the amount of data the satellite needs to transmit is larger then the amount it can transmit during one pass it needs to transmit it over several passes. Even if the amount of data is small it is possible that the satellite needs to retransmit the last frames which where not acknowledged during the last pass, if such frames exist. The AX.25 protocol discards the buffered data when a connection is lost.

To solve this problem we need a system which keeps track of which data are transferred and can be erased from memory, and which data it need to keep in memory until next time the satellite can transmit. This system must be implemented in a higher layer.

A property that AX.25 lacks is the ability to handle priorities. All data is transmitted in the order it is sent to the TNC. Prioritation between different data sources in the satellite must also be implemented in the OBC. It is possible to send UI-frames and thereby avoiding the normal flow control, but this is a very unreliable procedure.

The AX.25 protocol supports connection oriented frames with I-frames, and connectionless frames with UI-frames. The connectionless mode can be used for the satellites beacon since this form of communication is one way only and need no acknowledge responses. The connection oriented mode will be used when a ground station asks for a connection.

2.6.2 CCSDS Protocol

The most used transmission protocol for professional satellite telemetry is the CCSDS protocol. In order to better understand and convey the relationships among the many Recommendations that CCSDS has developed, as well as other standards that might be used, effort is underway to establish a methodology for representing end-to-end data system architectures. This methodology, a high level functional architecture, serves several purposes:

- it places each standard in its context to the total data system
- it allows potential users of the standards to quickly identify, for a given domain of interest, those standards that obtain at an appropriate system interface
- it indicates where gaps/overlaps in the total data system development effort may be forming
- it highlights standard interfaces so that modularized functions can be considered
- it promotes industry's interest in developing standard products for these (or other modules) through which the acceptance of standards can be furthered and the benefits of standards can be realized [Ccs].

The approach is to represent the overall system as a small set of boxes in which various high level functions are performed. The boxes are connected by arrows which indicate needed data/metadata flows at the interfaces between the functions. The data/metadata flows can be characterized by the set of standards to which they do/can/must conform.

It is worth emphasizing that the model is meant to highlight the methodology first, and only secondarily, the actual functional breakout shown. The model does not represent a rigid architecture that ties the hands of standards developers. Rather, it presents a framework that can be moulded to meet developers views and match manufacturers capabilities.

What is perceived for this model is a growing framework, growing in the sense of additional breakouts of detailed functions and services and protocols, that captures the current and future requirements of space endeavours civil, military, and commercial.

Funktional Model Diagram

The diagram below depicts the functional units (rectangles) and interfaces (circles) of the CCSDS Space Data System. This model is a top level model meant to depict the interfaces described in the CCSDS Blue Books.

It should be noted that there are other model views used by the CCSDS panels to depict various aspects of the overall space data systems in use by the CCSDS member agencies.

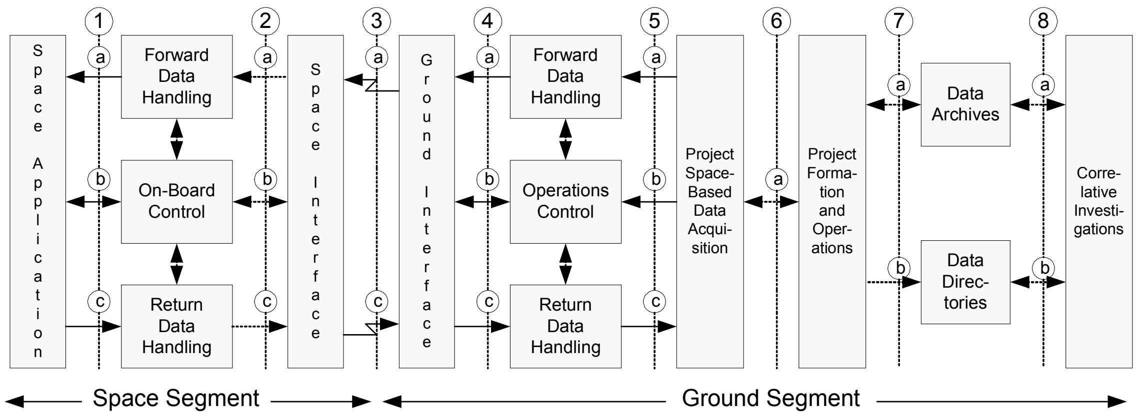

Figure 2.23: Space Data System Functional Model

Protocol Layer Model

The model is a five-layer model sometimes used to represent the protocol layers of Internet-type data communication. It is a simplification of the OSI seven layer model, with the OSI session and presentation layers omitted.

Existing CCSDS Recommendations for space data system protocols and services designed for use on the space link (the communications link between a spacecraft and ground station) are shown in blue. The Internet protocols, in grey, are included to show

how they fit into the CCSDS protocol stack when used in conjunction with the CCSDS Link and Physical layers [RVT01].

In addition to the protocols and services identified in the model, the CCSDS is developing a suite of SLE services designed to extend the space link, specifically, to enable spacecraft control and data acquisition from terrestrial locations remote from the ground station terminus of the space link. The organization has also developed Recommendations for a wide array of data description and archiving standards to support end-user handling and storage of telemetry data.

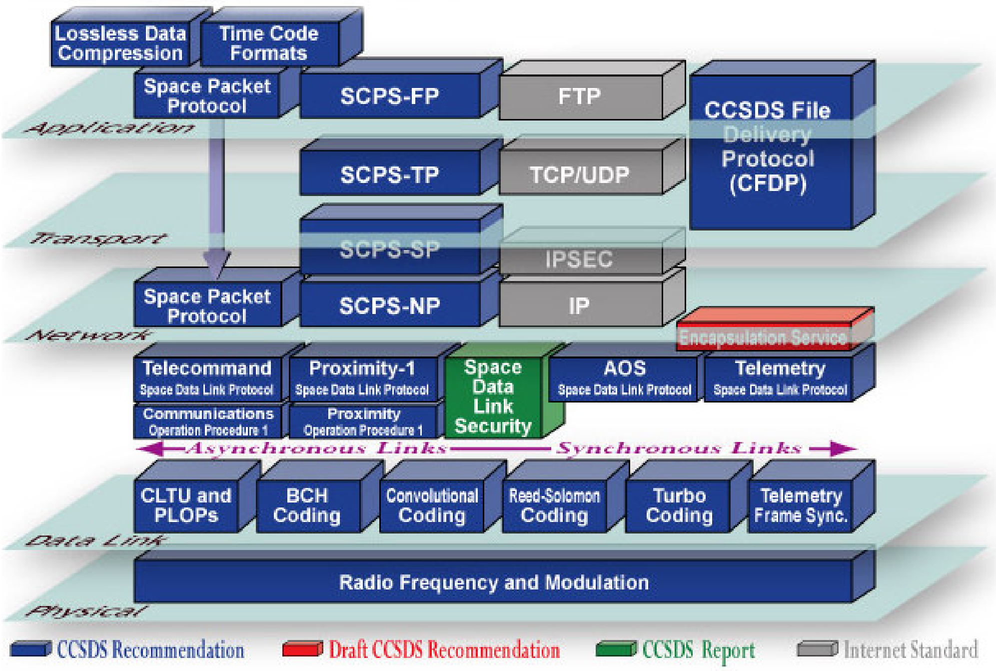

Figure 2.24: Protocol Layer Model

3 Design of a GPS Scintillation Payload

As shown in Chapter 1.3 the payload of the ACS consists of three scientific payloads. A FPGA experiment, a on board camera and a GPS szintillation experiment. Further will the ACS have a active attitude control system with magnetic torque coils and a real-time 3-dimensional navigation system.

The GPS scintillation experiment of the ACS is to obtain a profile of ionosphere plasma densities. One of the techniques will be GPS scintillation, where GPS signal strength at a point at two different times is compared. To achieve this, the satellite will be required to fly a GPS receiver and antenna. For simplification of the system, only one GPS antenna and receiver (for the navigation system and the scintillation experiment) will be implemented.

3.1 GPS, Ionosphere

The Global Positioning System, usually called GPS, is the only fully-functional satellite navigation system. A constellation of more than two dozen GPS satellites broadcasts precise timing signals by radio to GPS receivers, allowing them to accurately determine their location (longitude, latitude, and altitude) in any weather, day or night, anywhere on Earth.

GPS satellites broadcast three different types of data in the primary navigation signals. The first is the almanac which sends coarse time information with second precision along with status information about the satellites. The second is the ephemeris, which contains orbital information that allows the receiver to calculate the position of the satellite at any point in time. These bits of data are folded into the 37,500 bit NM, which takes 12.5 minutes to send at 50 Hz.

The satellites also broadcast two forms of accurate clock information, the C/A code, and the P code. The former is normally used for most civilian navigation. It consists of a 1,023 bit long pseudo-random code broadcast at 10.23 MHz, repeating every millisecond. Each satellite sends a distinct C/A code, which allows them to be identified. The P code is a similar code broadcast at 10.23 MHz, but it repeats only once per week. In normal operation, the so-called "anti-spoofing mode", the P code is first encrypted into the Y code, or P(Y), which can only be decrypted by units with a valid decryption key. All three signals, NM, C/A and P(Y), are mixed together and sent on the primary radio channel, L1, at 1575.42 MHz. The P(Y) signal is also broadcast alone on the L2 channel, 1227.60 MHz. Several additional frequencies are used for unrelated purposes, like L3 (1381.05 MHz), L4 (1841.40 MHz) and L5 (1176.45).

The **Ionosphere** is the part of the atmosphere that is ionized by solar radiation. It plays an important part in atmospheric electricity and forms the inner edge of the magnetosphere. It has practical importance because, among other functions, it influences radio propagation to distant places on the Earth [Ion].

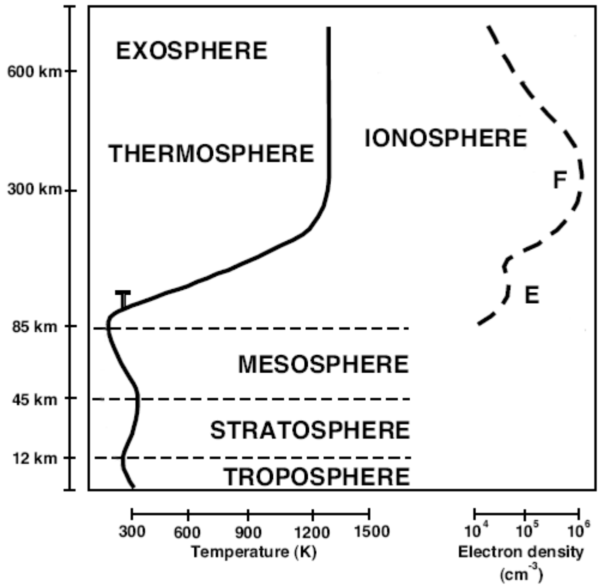

Figure 3.1: Relationship of the atmosphere and ionosphere

Solar radiation, acting on the different compositions of the atmosphere with height, generates layers of ionization:

- D Layer: The D layer is the innermost layer, 50 km to 90 km above the surface of the Earth.
- E Layer: The E layer is the middle layer, 90 km to 120 km above the surface of the Earth.
- E_S Layer: The Es layer or sporadic E-layer. Sporadic E propagation is characterized by small clouds of intense ionization, which can support radio wave reflections from 25 – 225 MHz.
- F Layer: The F layer or region, also known as the Appleton layer, is 120 km to 400 km above the surface of the Earth. Here extreme ultraviolet (10-100 nm) solar radiation ionizes atomic oxygen. The F region is the most important part of the ionosphere in terms of HF communications. The F layer combines into one layer at

night, and in the presence of sunlight (during daytime), it divides into two layers, the F1 and F2. The F layers are responsible for most skywave propagation of radio waves, and are thickest and most reflective of radio on the side of the Earth facing the sun.

3.2 Ionospheric Scintillation

Radio scintillations due to presence of moving irregularities in the ionosphere is a major problem in Navigation applications using GPS and in satellite communications, the problem being particularly acute around equatorial anomaly peak region Scintillation refers to rapid phase and amplitude fluctuations of the radio signals observed on or near the earth’s surface. Statistically, scintillation tends to be most severe at lower latitudes (within + 20 degrees of the geomagnetic equator) due to ionospheric anomalies in that region. It is also strongest from local sunset until just after midnight, and during periods of high solar activity. If sufficiently intense, these fluctuations can dramatically impact the performance of space-based communication and navigation systems. Ionospheric scintillation is the most significant disturbance that can affect GPS users during years of high sun spot activity. In the presence of scintillation, ionospheric modelling can be rendered impractical and receiver performance can be severely degraded. The influence of the ionosphere and a strategy to isolate its effect are issues of major concern for GPS positioning and navigation applications.

The worst source of scintillation is at the equatorial anomaly region, which corresponds to two belts, each several degrees wide, of enhanced ionization in the flayer at approximately 150 N and 150 S of the magnetic equator. In this region, during the solar cycle maxima periods, amplitude fading at 1.5 GHz may exceed 20 dB for several hours after sunset [BMB88].

The ionosphere affects GPS receivers by degrading the signal performance, in some cases causing loss of carrier lock, and by degrading the accuracy of differential corrections. These effects are caused by irregularities of electron density which scatter radio waves at L Band frequency and generate amplitude and phase scintillation. Amplitude scintillation causes cycle slips and data losses to occur and phase scintillation generate fast variation of frequency with which the receiver has to cope. Amplitude scintillations induce signal fading and, when this exceeds the fade margin of a receiving system, message errors in satellite communications are encountered and loss of lock occurs in navigational systems. The nominal C/No ratio for the L1 signal is about 45 dB/Hz, and tracking may be interrupted when C/No is less than 24 dB/Hz. It will be worse for the L2 signal because its power is 6 dB lower than that of L1. During periods of intense scintillation, the availability of carrier phase observations may be limited through loss of signal lock, with a significant impact on precise positioning applications. Such effects have a larger impact on the L2 tracking performance, where codeless and semi codeless technologies are employed to extract the encrypted L2 signal. The tracking performance of a given receiver depends not only on the magnitude of scintillation activity observed, but also on the receiver tracking capabilities.

The reduction in the number of simultaneously useable GPS satellites may result in a potentially less accurate position fix. Since scintillation occurrence is positively correlated with solar activity and the GPS network has received wide-spread use only recently during a quiet portion of the 11 year solar cycle, the true environmental vulnerability of the GPS constellation is yet to be observed. But even during low solar activity levels, it has been shown, under strong scintillation, that the GPS signals cannot be seen through the background noise due to the rapid changes in the ionosphere, even with the use of dual frequency receivers.

Several researchers have studied the impact of scintillation on GPS receiver performance [KF88]. Some studies have showed that ionospheric scintillation causes degradation in the GPS navigational accuracy and limitations in GPS receiver tracking performance [SKJ01]

3.3 GPS Scintillation Payload

One of the biggest problems for GPS accuracy is that changing atmospheric conditions change the speed of the GPS signals unpredictably as they pass through the ionosphere (see Chapter 3.2). The effect is minimized when the satellite is directly overhead and becomes greater toward the horizon, since the satellite signals must travel through the greater "thickness" of the ionosphere as the angle increases. Once the receiver's rough location is known, an internal mathematical model can be used to estimate and correct for the error.

Because ionospheric delay affects the speed of radio waves differently based on their frequencies, the second frequency band (L2) can be used to help eliminate this type of error. Some military and expensive survey-grade civilian receivers can compare the difference between the P(Y) signal carried in the L1 and L2 frequencies to measure atmospheric delay and apply precise corrections. This correction can be applied even without decrypting the P(Y) signal, as long as the encryption key is the same on both channels. In order to make this easier, the military is considering broadcasting the C/A signal on L2 starting with the Block III-R satellites. This would allow a direct comparison of the L1 and L2 signals using the same circuitry that already decodes the C/A on L1.

The effects of the ionosphere are generally slow by changing and can easily be tracked. The effects for any particular geographical area can be easily calculated by comparing the GPS-measured position to a known surveyed location. This correction, say, "10 meters to the east" is also valid for other receivers in the same general location. Several systems send this information over radio or other links to the receivers, allowing them to make better corrections that a comparison of L1 and L2 alone could. The amount of humidity in the air also has a delaying effect on the signal, resulting in errors similar to those generated in the ionosphere but located much closer to the ground in the troposphere. The areas affected by these problems tend to be smaller in area and faster moving than the billows in the ionosphere, making accurate correction for these effects more difficult.

3.3.1 Payload Requirements

The GPS board should receive a signal from the antenna, conditions and processes the signal into amplitude and location, and sends the data, with a time stamp, to the Command and Data Handling unit. The Antenna receives the GPS signal and transmits it to the GPS board.

The entire GPS system will be wired in the form of Figure 3.2.

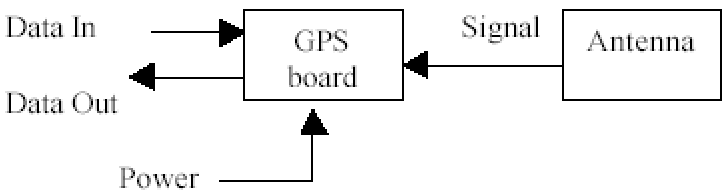

Figure 3.2: Block Diagram Requirements

Data In is the signal from Command and Data Handling to turn on or turn off. Data Out is the transmitted data to Command and Data Handling in the form of amplitude, location, and time. Signal is the non-amplified direct signal from the antenna and the power is 5 V from the power system.

The GPS board must fit in an box 9 cm by 9 cm by 2.1 cm high. The weight of the board itself must be 80 g or less. The Antenna must be a patch antenna able to be mounted on the surface of the spacecraft. The weight must be 10 g or less, covering an area less than 20 mm by 20 mm. The weight of the GPS board, antenna, and support-

ing components must not weigh more than 100 g, as dictated by the CubeSat Systems Specifications (see Appendix A).
The best candidates for the GPS board and antenna are:

Cornell Cougar Board
Weight = 39 g
Dimensions = 9.525 cm by 5 cm by 1.7 cm
Average Power 300 mA at 5V +/- .25 Volts
Electrical Interface: 0/5 Volt TTL level RF connector
Flight experience on Sounding rockets
Sampling Rate: Currently 50Hz)
The unit meets the specifications except for dimension. The 9.525 length is too long. An option is to adjust the internal cube configuration to accommodate the board. The Cougar does require a signal amplification of 20 to 35 dB from the antenna. The antenna subsystem does not content an LNA so this will have to be done on a board external from the antenna. This will add weight, but seeing as the GPS board is specified to have 80 g, this allows at least 40 g to work with. A simple amplifier would only weigh a few grams. In addition, the power aspect will have to be looked at, but the half watt clearance between the appropriated 2 W and the 1.5 W the Cougar draws should be adequate.

Toko DAX Dielectric Patch Antenna
Size is 18 mm x 18 mm x 4.5 mm.
Given the small size, it should weigh less than the specified 10 g. However, the thermal conditions, signal loss, and space worthiness must be tested.

Figure 3.3: GPS Patch Antenna [Cha01]

3.4 Disscusion

To carry out this scintillation experiment a few points have to been noted:

- Installed, programmed and sealed into the CubeSat, the GPS board and the antenna must perform correctly without maintenance.
- The irregularities in the F-layer of the ionosphere are ranging from 200 to 1000 km. The primary disturbance region are typically between 250 and 400 km. The maximum operation orbit of the CubeSat is 400 km.

The collected data are:

$$A_r \quad (A_r = A_o * \partial A)$$

$$A_r \ldots Amplitude\ of\ the\ received\ signal$$

$$A_o \ldots Nominal\ amplitude\ of\ the\ signal$$

$$\partial A \ldots Amplitude\ scintillation\ (affects\ directly\ the\ C/N_o)$$

and

$$\Phi_r \quad (\Phi_r = \Phi_o * \partial\Phi)$$

$$\Phi_r \ldots Phase\ measurement$$

$$\Phi_o \ldots Nominal\ phase$$

$$\partial\Phi \ldots Phase\ scintillation$$

After the data collection and the transmission to the ground station the scintilation effects on a GPS signal (in the worst case a error of ±10 m) can be calculated. For this the C/N_o and the phase of L1 (C/A, P(Y)) and L2 (P(Y) would be compared [FHR00] (example see Figure 3.4).

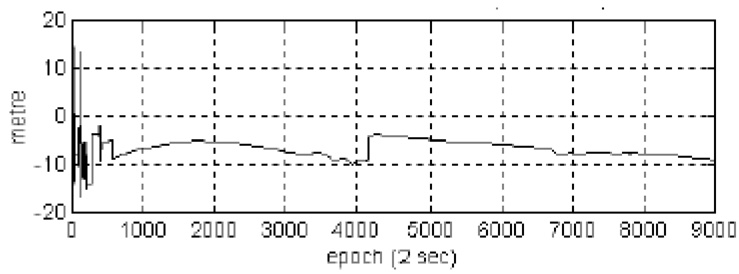

Figure 3.4: L1 Phase minus L2 Phase

4 Link Budget, Tracking

In order to calculate a possible scenario for this CubeSat Mission, the following defaults are given:

- Frequency should be 2190 MHz.
- The satellite shall operate in a 800 km circular (i=0°) or SSO (i=87°) orbit.
- Distance to satellite: 3293.18 km at horizon (slant range).
- Data transmission with a speed of 32/256/512 kbit/s and 1 Mbit/s.
- The CubeSat is equipped with an dipole antenna, a transmitter featuring a system noise temperature of 513 K and an maximum output power of 0.5 W.
- Further the CubeSat will be equipped with a 0.5 W (-3 dBW) transmitter feeding an dipole antenna, thus the antenna gain is 0 dB in the direction of the ground station and the satellite at horizon.

For the ground station, three different antennas are used:

- 0.7 m parabolic antenna, efficiency of 50%, G_r=21.10 dB, $\frac{G}{T} = -0.94\frac{dB}{K}$.
- 2.3 m Van mountable parabolic antenna (Andrews antenna), efficiency of 50%, G_r=31.47 dB ($G_r = 10\log\left(0.5\frac{\pi^2 2.3^2}{\left(\frac{3E8}{2.2E9}\right)^2}\right)$), $\frac{G}{T} = 9.43\frac{dB}{K}$ (antenna of the Graz University of Technology).
- 3 m parabolic antenna (*KTI* Mesh antenna), efficiency of 50%, G_r=33.74 dB, $\frac{G}{T} = 10.96\frac{dB}{K}$.

A transceiver (Radyne DMD 20) with a system noise temperature of 160 K and an output power of 100 W is assumed.

For the tracking of the Ground Station antennas three different tracking programmes types can be used (see Chapter 4.1).

Sun Synchronous Orbit

SSO means that a satellite pass over each area of the Earth's surface at a constant local time of day called local solar time. To achieve this condition, the orbit cannot exactly follow a true north-south track to go over the poles. Actually, the orbit must be slightly tilted towards the northwest with a steep inclination angle of about 98º. With the sun synchronous orbit, at any given latitude the position of the sun in the sky as the satellite passes overhead will be the same within the same season. This ensures consistent illumination conditions when acquiring images in a specific season over successive years, or over a particular area over a series of days. This means that a satellite can make repeated global observations from a single set of sensors with similar illumination from pass to pass. This is an important factor for monitoring changes between images or for mosaicing adjacent images together, as they do not have to be corrected for different illumination conditions.

Typically, equatorial crossing times of satellites are selected to avoid early morning mists or afternoon cloud in the tropics, to take advantages of the diurnal heating and cooling cycle in thermal infrared studies, or to ensure a low sun angle that highlights topographic features.

4.1 Tracking

A satellite tracking program is a computer program that predicts the position of a satellite using a mathematical model of the orbit. In other words it tells you where to aim the antennas so that they are pointing at the satellite.

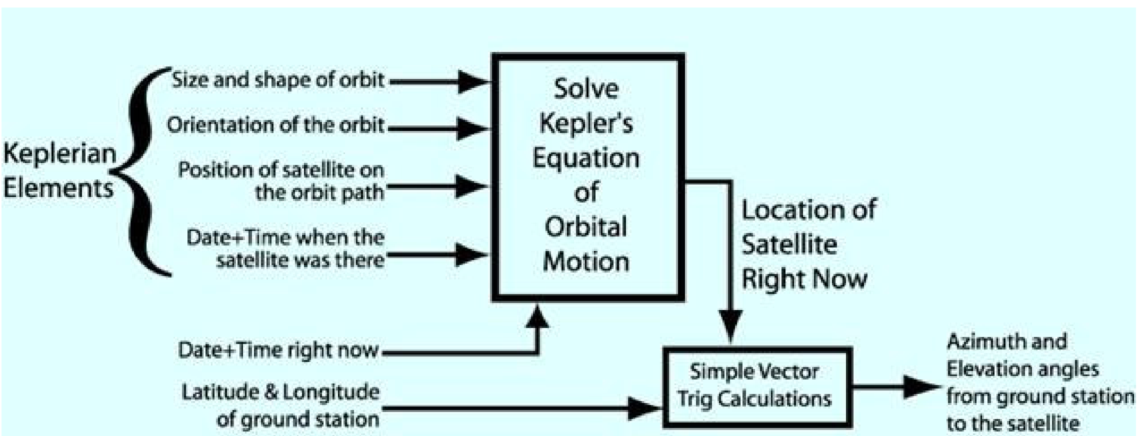

Figure 4.1: Tracking Model

As shown above, the satellite tracking program takes three kinds of input:

- **Keplerian Elements describing the satellite's orbit**
- **The current date and time**

In real time mode, the satellite tracking program obtains the current date and time from the computer's clock to be set in UTC to comply with the orbital elements.

The position on the Earth's surface of your station

There is no standard way for a program to find out geographic location, so you have to enter this information yourself, but only once. The program stores your location (and perhaps other locations you have entered), and automatically uses it next time you run the program.

From Kepler's Laws, we know that the orbit of a satellite is always an ellipse, with the center of the Earth at one focus. We also know how the speed of the satellite will vary as it moves around the orbit.

A set of Keplerian elements is a set of six or seven numbers that together define the size and shape of the ellipse, the orientation of the ellipse in three-dimensional space with respect to the Earth, and the location of the satellite on that ellipse at a particular time. With these numbers, the program can compute the location in three-dimensional space for any particular time.

Once the program has computed the location of the satellite, and you have told it the position of your ground station, it is a simple matter for the program to compute the direction from your station to the satellite. It expresses this direction in terms of Azimuth and Elevation. Azimuth is the horizontal direction (0 degrees is North, 90 degrees is East, and so on). Elevation is the angle from horizontal (0 degrees) to vertical (90 degrees). These angles are the most convenient form for pointing antennas, since we usually have separate azimuth and elevation rotators on our antennas.

A basic satellite tracking program will simply display the answers on the screen. This can be done in real time, or for some other particular time, or in a table of predictions for many times. Some programs are capable of passing the azimuth and elevation information to a rotor driver, which automatically controls the antenna rotors in order to keep them pointed at the satellite continuously.

4.1.1 Antenna Tracking Program

For the Graz University of Technology Ground Station (Figure 4.2) three tracking programms have been considered:

- NOVA for Windows
- Sat PC32 for Windows
- SCRAP

Further there are many other tracking programms (eg. MacDoppler Pro for Macitntosh, or PocketSat for Palm and Palm PC) are existing.

NOVA for Windows is a good choice.

NOVA for Windows

Nova for Windows is an innovative map based satellite tracking system. It features over 150 realistic 256 color and 16 bit color maps, unlimited numbers of satellites, observers, and views, as well as real-time control of antennas through several popular hardware interfaces [Owe00].

ARS is a powerful, low cost universal rotor interface. It can be connected to any rotor with several different ADC resolutions supported (8 & 10 bits). It supports a large list of log, contest, satellite tracking, and EME programs to control the azimuth and/or azimuth & elevation rotor unit.

ARS supports the most operating systems (DOS, Windows 3.x, Windows 9x, ME, Windows NT, Windows 2000, Windows XP and Linux) [Ea4].

The system consists of:

- RCI Board

This board is available for Azimuth or Azimuth and Elevation operation with all the components on the same PCB. It is connected to the computer via a LPT port.

- ARSWIN

ARSWIN will allow you to control your satellite tracking system. Several satellite trackers are supported. The elevation control option (RCI-SE or RCI + RCI-EL) is mandatory for satellite tracking.

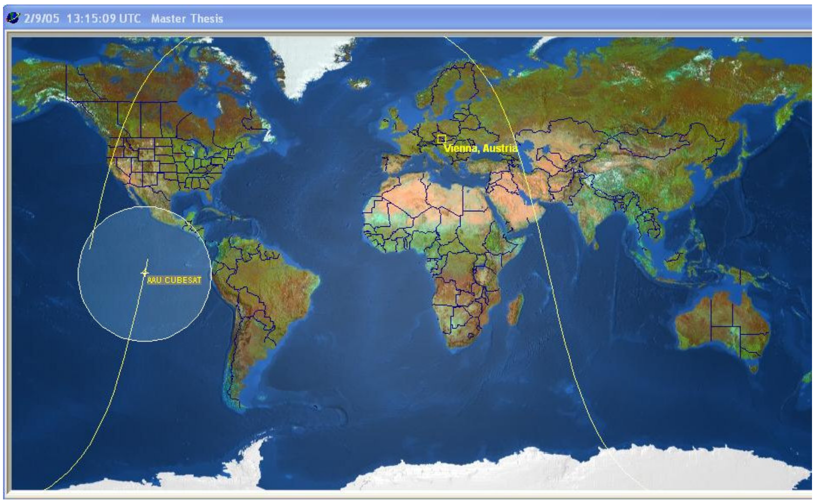

Figure 4.2: Rectangular Map - AAU CubeSat

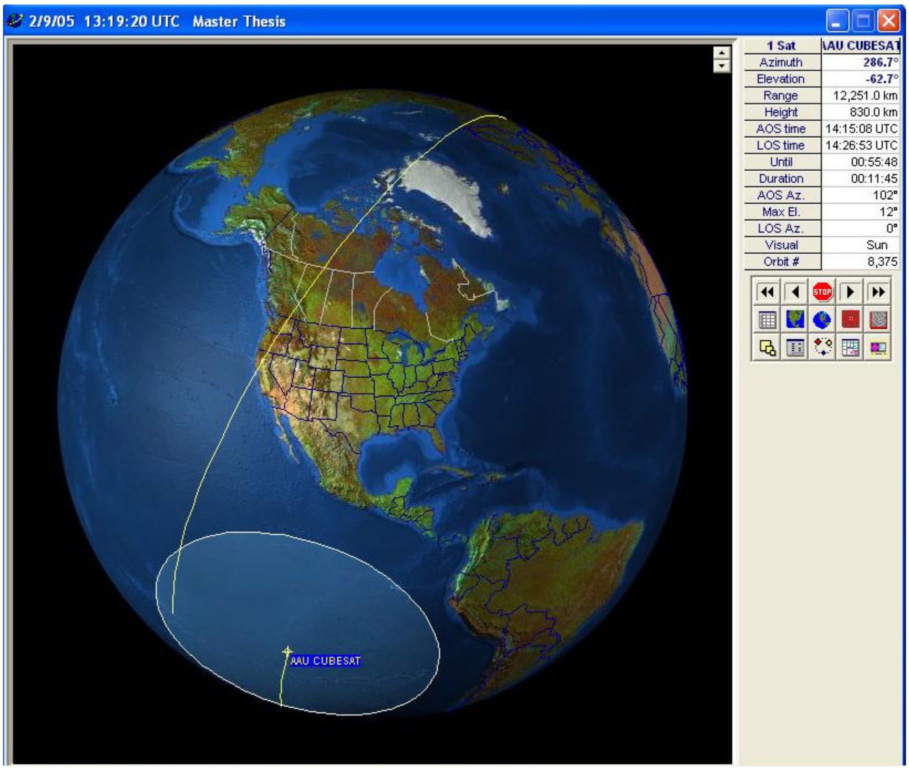

Figure 4.3: View from Space - AAU CubeSat

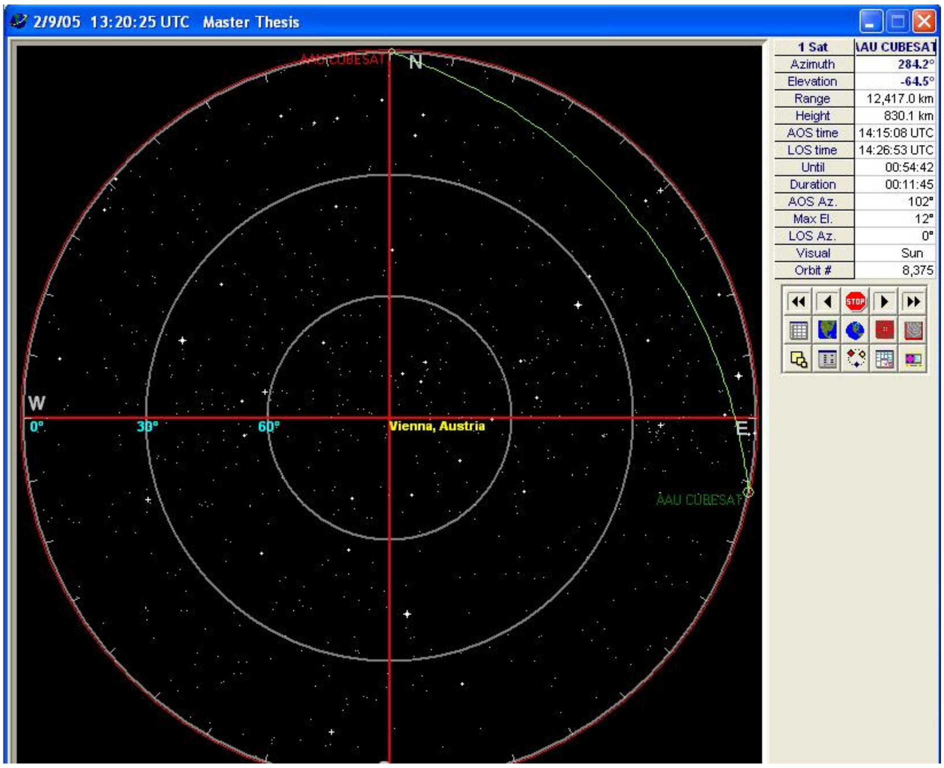

Figure 4.4: Radar Map - AAU CubeSat

4.2 **Link Budget**

An isotropic radio transmitter radiates its power P_t equally in all directions (isotropically). At a given distance d from the transmitter, the transmitted power is distributed equally on the surface of a sphere with a radius d and an area $4\pi d^2$. The flux density S in W/m^2 of an isotropically radiating antenna at a given distance d can be calculated using the following formula:

$$S = \frac{P_t}{4\pi d^2}$$

The fact that the satellite antenna will have some directivity, therefore the emitted power will be concentrated into a certain direction. Because of this, less than the full surface area of this sphere (4π steradian) will be "illuminated". The ratio between the full 4π steradian spherical coverage and the actually illuminated solid angle is called the Directivity and assumes that power is evenly distributed over and zero outside this area.

More important is the so-called Antenna Gain (G), which is the ratio of the flux density in a specific direction at a distance d and the flux density from the same transmitter using a hypothetical isotropic antenna.

At the receiving antenna, called "effective area" is assumed, in order to calculate the amount of electromagnetic energy received. Using this Effective Area (A_r), it is possible to calculate the total collected power $P_r = SA_r$.

A receiving antenna has an antenna gain like a transmitting antenna, which is related to A_r.

$$A_r = \frac{\lambda^2}{4\pi} G_r$$

In this formula λ refers to the wavelength of the transmitted signal and G_r is the antenna gain of the receiving antenna. In addition to this formula it can be theoretically proven that the transmitting and receiving antenna gain is the same for the same antenna at the same frequency.

The antenna gain depends on the antenna design; while parabolic antennas feature antenna gains of 60 dB and more, a Yagi-type antenna has an antenna gain of some 20 dB (depending on the number of directing - elements in the design) and an dipole antenna has an antenna gain of 2 dB.

Derivation of the Link Budget

The link budget is the foundation for designing any radio link, regardless if it is terrestrial or in space. Putting the considerations presented in Section 4.2.1 into one single equation, it is possible to express to relationship between the transmitting power and the power at the output terminal of the receiving antenna, based on the formula for the collecting power $P_r = S\,A_r$.

$$\begin{aligned} P_r &= \frac{P_t G_t}{4\pi d^2} A_r \\ &= \frac{P_t G_t}{4\pi d^2} \frac{\lambda^2}{4\pi} G_r \\ &= \left(\frac{\lambda}{4\pi d^2} \right) P_t G_t G_r \\ &= \left(\frac{c}{4\pi d f} \right)^2 P_t G_t G_r \end{aligned}$$

The quantity $\left(\frac{c}{4\pi d f} \right)^2$ is also denoted L_P^{-1} and is called the Path Attenuation or Path *Loss*, a dimensionless quantity. Using this Path Loss, the relationship between the received and transmitted powered may now be simply expressed with:

$$\frac{P_r}{P_t} = \frac{G_t G_r}{L_P}$$

It is more convenient to express the link budget in decibel (dB), mathematical calculations become more easily (a multiplication transforms into an addition and a division into a subtraction). Because it is not allowed to take the logarithm of a dimensioned quantity, a reference power has to be selected, 1 Watt is very suitable for this:

$$10\log\frac{P_r}{1W} - 10\log\frac{P_t}{1W} = 10\log G_r - 10\log L_P[dB]$$

Moving into *dB* simplifies this equation:

$$P_r - P_t = G_t + G_r - L_P[dBW]$$
$$P_r = P_t + G_t + G_r - L_P[dBW]$$

It is possible to transform the path attenuation, into dB as well, resulting in a formula depending on the distance and frequency:

$$L_P = 32.34 + 20\log\frac{S}{1[km]} + 20\log\frac{f}{1[MHz]}$$

32.34 dBW contains the constant $\frac{4\pi}{c}$ as well as the power of 10 due to the more convenient usage of kilometres instead of meters for the distance and Megahertz instead of Hertz for the carrier frequency. The final formula for the link budget can now be given:

$$P_r = P_t + G_t + G_r - 32.45 - 20\log\frac{s}{1[km]} + 20\log\frac{f}{1[MHz]}$$

Slant Range

Although a perfect circular orbit is assumed, which makes the height of the CubeSats orbit constant, the distance between the satellite is not constant (see Figure 4.5). In order to simplify calculations, a perfectly spherical earth with a radius Re = 6378.136 km is assumed as well. For our calculation we assume a orbit height of h = 800 km.

The maximum distance between the ground station and the satellite with communication being possible occurs when the satellite is just over the horizon (δ=0 degrees). If it is below the horizon, no communication is possible, if the satellite moves up, the distance is decreasing until it reaches the zenith. Using the law of Pythagoras it is now possible to calculate the distance between the satellite and the ground station at this moment:

$$s = R_e[\{\frac{r^2}{R_e^2} - \cos^2(\delta)\}^{\frac{1}{2}} - \sin\delta] = 3293.18km$$

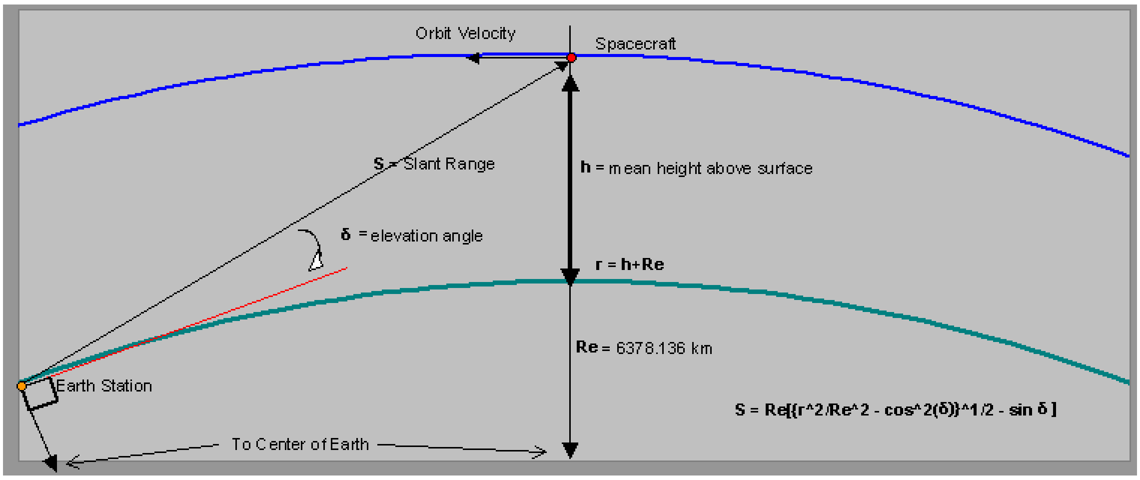

Figure 4.5: Slant Range

It is now possible to calculate the path loss in this scenario for any given frequency:

Frequency f [MHz]	Path Loss L_P [dB]
135	145.4
145	146.0
450	155.9
2190	169.6

Table 4.1: Free Space Loss for a Number of given Frequencies

Thermal Noise

It is not only the path loss or the link budget, which determines whether a communications link is reliable or not, a very important role plays Thermal Noise. Every electronic device is producing this thermal noise, limiting how small a signal may be to be detected. Thermal noise is not only generated inside electronic devices, but the antenna looking into the sky captures galactic noise, the cosmic background radiation, and noise from the attenuation of the radio waves passing through the atmosphere caused by water vapor.

In the theory of thermodynamics, noise calculations are related to power considerations. An ideal ohmic resistor in thermal equilibrium at an absolute temperature T will produce an ”available noise power” P_N given by:

$$P_n = kTW = N_0 W$$

In this formula, k is Boltzmann's constant $k = 1.38062 \cdot 10^{-23} \frac{J}{K}$, W is the bandwidth of the frequency band containing the signal of interest and $N_0 = kT$ is the noise spectral density, having the unit Watt per Hertz of bandwidth and denotes the noise power in a 1 Hz band.

For this task all calculations of noise figure are related to a universally accepted reference noise temperature T_0 = 290 K. The noise temperature of a two-port is defined to be $F = \left(\frac{S}{N}\right)_{IN} / \left(\frac{S}{N}\right)_{OUT}$.

The corresponding noise temperature is calculated by considering all the noise as coming from a resistor at temperature T_e at the input of the two-port and the two-port itself as being noiseless. Thus it can be derived that:

$$T_e = T_0(F-1)$$
$$F = 1 + \frac{T_e}{T_0}$$

Because the noise temperature for a purely resistive loss L is given by $T_L = T_0(L-1)$, the total receiver noise temperature can now be calculated:

$$T_{RX} = T_0(L-1) + LT_{LNA} + \frac{L}{G_{LNA}} T_2 [K]$$

In many cases N_0 is a constant regardless of frequency and the noise thus denoted "white noise" in analogy to white light that contains an equal amount of light at all wavelengths. The noise in a radio receiver consists of many different contributions. These are often all referred to an interface at the antenna terminals including the noise from the antenna itself. All noise contributions are expressed as "noise temperatures" and the sum is denoted the "system noise temperature" T_{sys} or just T for short. The total noise power at the receiver input is therefore:

$$P_n = P_{n,sys} = kT_{sys}W = ktW = k(T_a + T_{RX})W$$

implying that $T_{sys} = T_a + T_{RX}$ is the sum of antenna and receiver noise temperatures.

Signal to Noise Ratio

The SNR is the ratio between the power of the information carrying signal and the power of the unwanted noise (in the same bandwidth): $SNR = \frac{P_s}{P_n}$ where P_S is the signal power and P_n is the noise power. In the dB-domain it can be expressed by:

$$SNR[dB] = P_S[dBW] - P_n[dBW]$$

Using the link budget equation $P_r = P_t + G_t + G_r - L_P$ previously derived, we get:

$$SNR = P_t + G_t + G_r - L_P - P_n$$

The value of the SNR is the determining factor whether we can extract useful information from the received radio signal or not. A formula for calculating the Signal-to-Noise Ratio can be defined, which expresses the energy per information bit divided by the noise spectral density:

$$\frac{E_b}{N_0} = \frac{P_s}{P_N} \cdot \frac{B_N}{r}$$

$r ... Information\ rate$
$B_N ... Noise\ bandwith$

Moving this equation into the dB-domain simplifies the expression, $\frac{E_b}{N_0}$ is now taken as a symbol and is expressed in dB, and P_r in dBW or dBm:

$$\frac{E_b}{N_0} = P_r - 10\log\frac{B_N}{1Hz} - 10\log\frac{k}{1J/K} - 10\log\frac{T}{1K}$$

Combining this formula with the link budget equation and denoting the quantity P_t +G_t as Equivalent Isotropically Radiated Power (EIRP) gives:

$$\frac{E_b}{N_0} = EIRP + G_r - L_P - 10\log\frac{B_N}{dBHz} - 10\log\frac{k}{dBJ/K} - 10\log\frac{T}{dBK}$$

Finally, the path loss L_P is added and the dB-value of *Bolzmann's* constant calculated, giving the final link budget equation:

$$\frac{E_b}{N_0} = EIRP + \frac{G}{T} + 196.15 - 20\log\frac{s}{1km} - 20\log\frac{f}{1MHz} - 10\log\frac{B}{1Hz}[dB]$$

EIRP = P_t+G_t is called the "Equivalent Isotropically Radiated Power" or the power required by the transmitter output stage if the antenna radiated equally in all directions (isotropically). The advantage of using EIRP is that it is possible to trade antenna gain for transmitter output power for a given EIRP requirement. $\frac{G}{T} = G_r - 10\log\frac{T}{1K}[dB/K]$, pronounced G-over-T (G/T) or Figure of Merit, is a measure of the quality factor or performance of the receiver and an important characteristic for both the satellite and the ground station. G/T allows the link designer to trade receiving antenna gain for system noise temperature with a given G/T requirement.

4.2.1 Link Calculations

This formula gives an ideal (optimistic) view regarding the losses occurring on a satellite link, but in reality additional losses have to be considered as well:

Output Losses: Losses occurring due to the electrical connection between the transmitter and the antenna.

Pointing Loss: This loss occurs because the antennas are not aligned perfectly.

Atmospheric Attenuation: Gases in the lower parts of the atmosphere absorb electromagnetic waves. This loss greatly depends on the rain rate, drop size and frequency.

In reality, these losses are about 2 to 3 dB in total, but especially the atmospheric attenuation varies greatly. The following calculations do not include these losses, but they are considered to be part of the link budgets remaining margin.

In order to calculate a possible scenario for this CubeSat mission, i got the following defaults:

- Frequency should be 2190 MHz.
- The satellite shall operate in a 800 km circular (i=0°) or *SSO* (i=87°) orbit.
- Distance to satellite: 3293.18 km at horizon (slant range).
- Data transmission with a speed of 9.6/32/256/512 kbit/s and 1 Mbit/s.
- The CubeSat is equipped with an omnidirectional antenna, a transmitter featuring a system noise temperature of 513 K and a maximum power output of 0.5 W.

For the ground station, three different antennas are used:

- 0.7 m parabolic antenna, efficiency of 50%, G_r=21.10 dB, $\frac{G}{T} = -0.94\frac{dB}{K}$.
- 2.3 m parabolic antenna (*Andrews* antenna), efficiency of 50%, G_r=31.47 dB, ($G_r = 10\log\left(0.5\frac{\pi^2 2.3^2}{\left(\frac{3E8}{2.2E9}\right)^2}\right)$), $\frac{G}{T} = 9.43\frac{dB}{K}$ $\left(31.47\,dB - 22.04\,dB\right)$.
- 3 m parabolic antenna (*KTI* mesh antenna), efficiency of 50%, G_r=33.74 dB, $\frac{G}{T} = 10.96\frac{dB}{K}$.

  All three antennas are fed by a transceiver (Radyne DMD 20) with a system noise temperature of 160 K and feature an output power of 100 W.

Downlink from the CubeSat to the Ground Station

The CubeSat will be equipped with a 0.5 W (-3 dBW) receiver feeding an omni-directorial radiating antenna, thus the antenna gain is 0 dB in the direction of the ground station and the satellite at horizon. For a frequency of 2190 MHz and different data rates we get link budgets for the three antenna types.

Data Rate [bit/s]	E_b/N_0 [dB], 0.7 m	E_b/N_0 [dB], 2.3 m	E_b/N_0 [dB], 3 m
9600	15.2	25.6	27.6
32000	10.0	20.3	21.9
256000	-	11.3	12.8
512000	-	8.3	8.9
1000000	-	5.4	6.9

Table 4.2: Downlink Signal-to-Noise-Ratio

Uplink from the Ground Station to the CubeSat

The same calculations can be performed for the uplink as well, which is needed to control the satellite (”Telecommand”). In this case, the ground station sends its signals with quite some high power using a directional antenna, and these signals have to be received by the small omnidirectional antenna of the CubeSat, featuring only a very bad $\frac{G}{T}$, further assumptions have to be made:

- Transmitter power output: 100 W (1 W, see Table 4.4)*
- $\frac{G}{T}$ of the satellite: -27 dB/Hz (system noise temperature of 513 K, $\frac{G}{T} = G_r - 10\log\frac{T}{1K} = 0 - 10\log\frac{513}{1}$)

Data Rate [bit/s]	E_b/N_0 [dB], 0.7 m	E_b/N_0 [dB], 2.3 m	E_b/N_0 [dB], 3 m
9600	33.1	43.6	45.8
32000	28.0	38.4	40.4
256000	19.0	29.4	31.6
512000	16.0	26.4	28.6
1000000	13.1	23.4	25.7

Table 4.3: Uplink Signal-to-Noise-Ratio

Data Rate [bit/s]	E_b/N_0 [dB], 0.7 m	E_b/N_0 [dB], 2.3 m	E_b/N_0 [dB], 3 m
9600	13.1	23.6	25.8
32000	8.0	18.4	20.4
256000	-	9.4	11.6
512000	-	6.4	8.6
1000000	-	3.4	5.7

Table 4.4: Uplink Signal-to-Noise-Ratio (1 W Transmitter Power Output)*

4.2.2 Modulations Schemes

In Chapter 4.2.1 the SNR for the uplink and downlink for 2190 MHz and different data rates were calculated. But the probability of correctly transmitting data not only depends on the SNR, but also on a possible coding scheme used.

One strategy to reduce the probability of erroneous transmission is called FEC. The transmitter adds an error-correcting code to the data block, which is transmitted to the receiver. This error-correcting code is a function of the data bits. Upon reception, the receiver calculates the error-correcting code from incoming data bits as well. If the calculated code matches the incoming code, no error occurred, and the data was received correctly. If the error-correcting codes do not match, the receiver attempts to determine the erroneous bits in error and correct them.

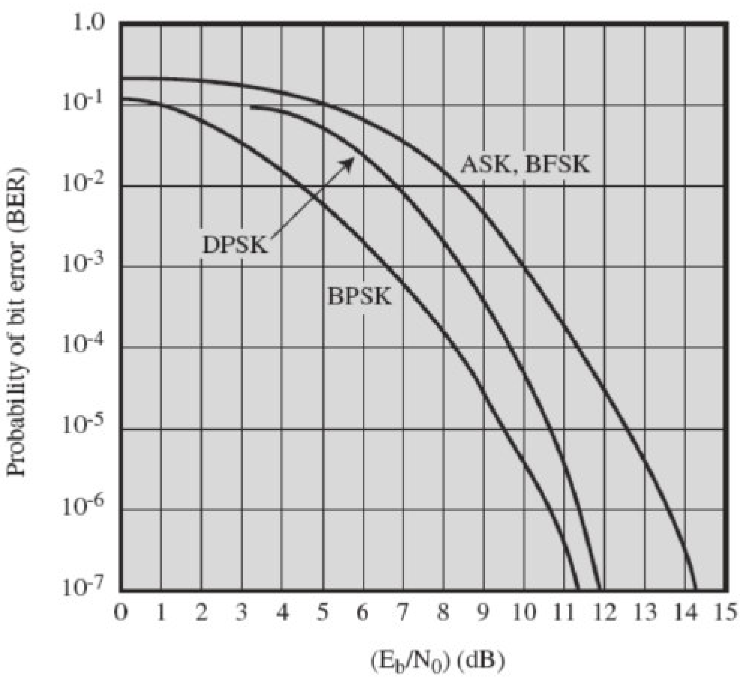

Figure 4.6: Performance of Different Modulations Schemes

Performance

A number of factors determine how successful a receiver will be interpreting an incoming signal. Particular parameters include the SNR, the data rate and bandwidth. An increase of the data rate increases the bit error rate. On the other hand, an increase in the SNR decreases the bit error rate.

But the modulation scheme itself also plays a key issue when talking about how successful an incoming signal can be interpreted. In Figure 4.6 the probability of BER is plotted against the SNR ($\frac{E_b}{N_0}$) for ASK, BFSK, BPSK and DPSK. It can be clearly seen that for a given SNR, a transmission using BPSK will produce a far lower BER then transmission using BFSK. On the other hand, in order to transmit data with a certain BER, a much higher SNR is needed when transmitting data with BFSK.

By encoding the data with coding schemes, the performance of the transmission can be increased. Depending on the parameters of the code used, for a given $\frac{E_b}{N_0}$ the BER will be much lower compared to un-encoded transmission.

On the other hand, in order to transmit data with a certain BER, a much lower $\frac{E_b}{N_0}$ is needed when transmitting un-encoded data. The difference of the two needed $\frac{E_b}{N_0}$ is called Coding Gain. Figure 4.7 shows the coding gain of different decoders. This diagram is based on PSK. For FSK, 3 dB have to be added to the SNR. Depending on the complexity of the decoder, a certain coding gain can be achieved compared to un-encoded transmission. At the left side of the diagraph, the Shannon Border is shown, a theoretical limit of the performance of a decoder. All the following calculations will be conducted for PSK only, for FSK additional 3 dB have to be taken into account, but the calculations itself stay the same.

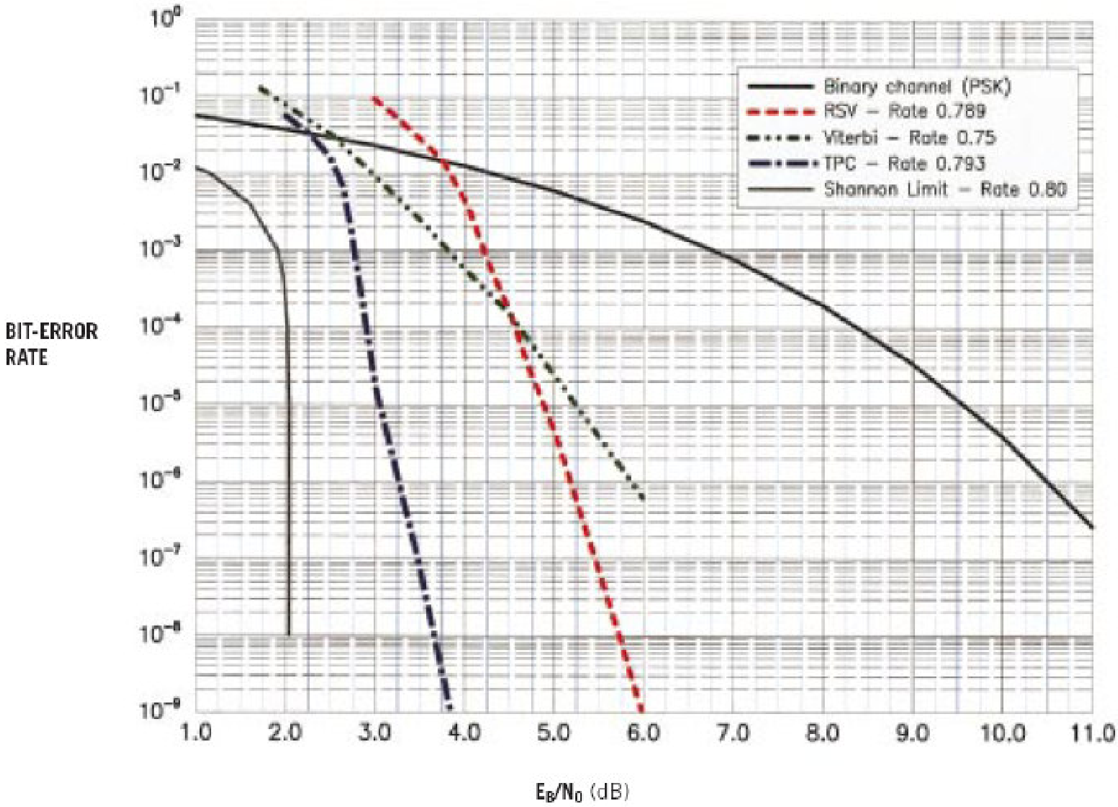

Figure 4.7: Coding Gain for Different Coding Techniques

4.2.3 Un-encoded Transmission

When not using any Forward-Error-Correction, the link-budget for the downlink channel does not tolerate a lot of additional losses. The calculated SNR of the downlink for a transmission frequency of 2190 MHz is budgeted with 15.02 dB (for 9600 kbit/s and a 0.7 m antenna), not including any additional losses, like atmospheric attenuation, depolarization-losses or pointing-losses. If a BER of 10^{-6} is desired, a SNR of at least 10.5 dB is required, leaving only a margin of 4.7 dB for all additional losses. But typical applications have shown these additional losses to be at least 3 dB (13.5 dB).

Data Rate [bit/s]	0.7 m Antenna		2.3 m Antenna		3 m Antenna	
	10^{-6}	10^{-9}	10^{-6}	10^{-9}	10^{-6}	10^{-9}
9600	4.7	1.7	15.1	12.1	17.2	14.1
32000	-0.5	-3.5	9.8	6.8	11.4	8.4
256000	-	-	0.8	-2.2	2.3	-0.7
512000	-	-	-2.2	-5.2	-1.6	-4.6
1000000	-	-	-5.1	-8.1	-3.6	-6.6

Table 4.5: Margin Downlink Un-encoded Transmission

Data Rate [bit/s]	0.7 m Antenna		2.3 m Antenna		3 m Antenna	
	10^{-6}	10^{-9}	10^{-6}	10^{-9}	10^{-6}	10^{-9}
9600	22.6	19.6	33.1	30.1	35.3	32.3
32000	17.5	14.5	27.9	24.9	29.9	26.9
256000	8.5	5.5	18.9	15.9	21.1	18.1
512000	5.5	2.5	15.9	12.9	18.1	15.1
1000000	2.6	-0.4	12.9	9.9	15.2	12.2

Table 4.6: Margin Uplink Un-encoded Transmission

For an un-encoded data transmission, SNR of **10.5 dB** is needed to achieve a BER of 10^{-6}, in order to achieve a BER of 10^{-9}, a SNR of **13.5 dB** is necessary (see Figure 4.7). When analyzing the data provided in the table above, it is obvious that the downlink channel is very critical when using un-encoded transmission. At 2190 MHz, the margin for all additional losses is 4.7 dB for a BER of 10^{-6}, respectively 1.7 dB if a BER of 10^{-9} shall be achieved.

The uplink is by far not as critical. Even at 2190 MHz a margin of 22.6 dB is left for a BER of 10^{-6} for a 9600 bit/s data rate and a 0.7 m dish. For a BER of 10^{-9}, a margin of 19.6 dB is left, more then enough to compensate additional losses occurring on the link.

4.2.4 Viterbi Code

For data transmissions using a Viterbi decoder, an SNR of **5.8 dB** is needed to achieve BER of 10^{-6}; in order to get a BER of 10^{-9}, a SNR of **7.3 dB** is required (see Figure 4.7). Compared to the un-encoded transmission, a SNR being about 4.8 dB lower is only required.

Data Rate [bit/s]	0.7 m Antenna		2.3 m Antenna		3 m Antenna	
	10^{-6}	10^{-9}	10^{-6}	10^{-9}	10^{-6}	10^{-9}
9600	9.4	7.9	19.8	18.3	21.8	19.4
32000	4.2	2.7	14.5	13	16.1	14.6
256000	-	-	5.5	4	7	5.5
512000	-	-	2.5	1	3.1	1.6
1000000	-	-	-0.4	-1.9	1.1	-0.4

Table 4.7: Margin Downlink Viterbi-Coded Transmission

Data Rate [bit/s]	0.7 m Antenna		2.3 m Antenna		3 m Antenna	
	10^{-6}	10^{-9}	10^{-6}	10^{-9}	10^{-6}	10^{-9}
9600	27.3	25.8	37.8	36.3	40	38.5
32000	22.2	20.7	32.6	31.1	34.6	33.1
256000	13.2	11.7	23.6	22.1	25.8	24.3
512000	10.2	8.7	20.6	19.1	22.8	21.3
1000000	7.3	5.8	17.8	16.3	19.9	18.4

Table 4.8: Margin Uplink Viterbi-Coded Transmission

According to the table shown above, the downlink is now by far less critical compared to the un-encoded transmission. Even at a frequency of 2190 MHz and a desired BER of 10^{-9} enough margin is left, which should be sufficient during normal weather conditions. If a BER of only 10^{-6} is required, the margin increases.

The same applies for the uplink, it is even less critical compared to the un-encoded transmission.

4.2.5 Turbo Code

For data transmission using a Turbo decoder, a SNR of **3.2 dB** is needed to achieve a BER of 10^{-6}, in order to achieve a BER of 10^{-9}, a SNR of **3.7 dB** is required (see Figure 4.7). Compared to the un-encoded transmission, a SNR being about 7.3 dB lower.

Data Rate [bit/s]	0.7 m Antenna		2.3 m Antenna		3 m Antenna	
	10^{-6}	10^{-9}	10^{-6}	10^{-9}	10^{-6}	10^{-9}
9600	12	11.5	22.4	21.9	24.4	23.9
32000	6.8	6.3	17.1	16.6	18.7	18.2
256000	-	-	8.1	7.6	9.6	9.1
512000	-	-	5.1	5.6	5.7	5.2
1000000	-	-	2.2	1.7	3.7	3.2

Table 4.9: Margin Downlink Turbo-Coded Transmission

Data Rate [bit/s]	0.7 m Antenna		2.3 m Antenna		3 m Antenna	
	10^{-6}	10^{-9}	10^{-6}	10^{-9}	10^{-6}	10^{-9}
9600	29.9	29.4	40.4	39.9	42.6	42.1
32000	24.8	24.3	35.2	34.7	37.2	36.7
256000	15.8	15.3	26.2	25.7	28.4	27.9
512000	12.8	12.3	23.2	22.7	25.4	24.9
1000000	9.9	9.4	20.2	19.7	22.5	22

Table 4.10: Margin Uplink Turbo-Coded Transmission

Even better margins are achieved when using a Turbo decoder compared to un-encoded transmission or transmission using a Viterbi decoder. At 2190 MHz and a desired BER of 10^{-9}, a margin of 11.5 dB is left in the SNR. Due to the characteristics of the coding scheme, when decreasing to BER to 10^{-6}, the margin increases.

No matter if the data is transmitted un-encoded or a FEC coding scheme is used, the downlink channel is by far more critical then the uplink channel, because at the ground station far more power is available and the transmitter features a lower noise temperature (it is more sophisticated, but also far more heavier). In order to transmit data at the downlink channel with an reasonable low BER (at least 10^{-6}, but 10^{-9} would be better) and allowing some additional losses to be present at the channel, some coding scheme is necessary, the performance of un-encoded data transmission is not sufficient. A Viterbi decoder would be sufficient, but a Turbo coder could provide an even higher margin, allowing greater losses on the downlink channel be present while still transmitting data successfully.

Summary

The aim of this thesis was to examine a communication and a GPS scintillation payload for a CubeSat, a follow up project of the Nano-Satellite TUGSAT-1 within the framework of the BRITE-Austria Mission.

Any satellite, which shall be considered being a CubeSat, must fulfill the requirements of the CubeSat-Standard defined by Stanford University and California Polytechnical Institute. This CubeSat Standard introduced at the very beginning, defines size, mass and mechanical as well as electrical specifications of these tiny research satellites with a size of 10 x 10 x 10 cm and weighing less than 1 kg. A large number of these satellites can be launched together in order to decrease launch costs, it is important that these satellites can easily be integrated into the launch vehicle and do not pose any danger amongst each other.

The first part of the thesis contains antenna and transceiver design for a frequency of 2.2 GHz. Other CubeSat satellites only use the very simple communication protocols like the AX.25 protocol, this CubeSat satellite shall utilize the CCSDS standard or the SRLL protocol for telemetry and telecommand. In order to support this, a brief presentation of this standard and protocol are first given. After this a complete calculation of a Hertzian dipole were made.

The result shows that a patch antenna is the best choice for this high frequency. But the small size (10 x 10 x 10 cm), the mass (1 kg) and the power consumption (no margin left) of this CubeSat permits only one antenna type. The only suitable antenna for this specially CubeSat is a $\frac{\lambda}{2}$ Dipole. Starting with this, Dipole calculations and antenna deployment specifications are made. In the end a suggestion for a suitable transceiver for the CubeSat mission were made.

One proposed experiment of the satellite is a GPS scintillation payload. GPS receiver tracking performance can be increased during periods of enhanced ionospheric activity, where small-scale scintillation effects (phase and amplitude variations) are observed in the high latitude auroral region and the low latitude equatorial anomaly region. During periods of intense scintillation, the availability of carrier phase observations may be limited through loss of signal lock, with a significant impact on precise positioning applications. Such effects have a larger impact on the L2 tracking performance, where codeless and semi codeless technologies are employed to extract the

encrypted L2 signal. With a a feasibility study of this Payload ends the second part of this thesis.

Concluding this thesis are calculations regarding the link budget for the up-link and downlink for three different antenna types. A 0.7 m parabolic antenna (G_r=21.10 dB), a 2.3 m Andrews antenna (G_r=31.47 dB) and a 3 m mesh antenna with G_r=33.74 dB. Various data rates (from 9.6 kbit/s to 1 Mbit/s) and the comparison of un-encoded transmission with encoded transmission with different coding schemes (Viterbi and Turbo code) shows the reliable communication between ground station and satellite.

Appendix A: CubeSat Specification

The primary mission of the CubeSat Program is to provide access to space for small payloads. The primary responsibility of Cal Poly as a launch coordinator is to ensure the safety of the CubeSats and protect the LV, primary payload, and other CubeSats. CubeSat developers should play an active role in ensuring the safety and success of CubeSat missions by implementing good engineering practice, testing, and verification of their systems. Failures of CubeSats, the P-POD, or interface hardware can damage the LV or a primary payload and put the entire CubeSat Program in jeopardy. As part of the CubeSat Community, all participants have an obligation to ensure safe operation of their systems and to meet the design and testing requirements outlined in this document [Tor05], [MHJ01].

P-POD Interface

The P-POD is Cal Poly's standardized CubeSat deployment system. It is capable of carrying three standard CubeSats and serves as the interface between the CubeSats and LV. The P-POD is an aluminium, rectangular box with a door and a spring mechanism. CubeSats slide along a series of rails during ejection into orbit. CubeSats must be compatible with the P-POD to ensure safety and success of the mission, by meeting the requirements outlined in this document. Additional unforeseen compatibility issues will be addressed as they arise.

General Responsibilities

- CubeSats must not present any danger to neighbouring CubeSats in the P-POD, the LV, or primary payloads:
  - All parts must remain attached to the CubeSats during launch, ejection and operation. No additional space debris may be created.
  - CubeSats must be designed to minimize jamming in the P-POD.
  - Absolutely no pyrotechnics are allowed inside the CubeSat.
- NASA approved materials should be used whenever possible to prevent contamination of other spacecraft during integration, testing, and launch.
- The newest revision of the CubeSat Specification is always the official version
  - Developers are responsible for being aware of changes.
  - Changes will be made as infrequently as possible bearing launch provider requirements or widespread safety concerns within the community.

- Cal Poly will send an update to the CubeSat mailing list upon any changes to the specification.
- CubeSats using an older version of the specification may be exempt from implementing changes to the specification on a case-by-case basis.

Cal Poly holds final approval of all CubeSat designs. Any deviations from the specification must be approved by Cal Poly launch personnel. Any CubeSat deemed a safety hazard by Cal Poly launch personnel may be pulled from the launch.

Dimensional and Mass Requirements

CubeSats are cube shaped Picosatellites with a nominal length of 100 mm per side. Dimensions and features are outlined in the CubeSat Specification Drawing (see Figure 0.1)

General features of all CubeSats are:

- Each single CubeSat may not exceed 1 kg mass.
- Center of mass must be within 2 cm of its geometric center.
- Double and triple configurations are possible. In this case allowable mass 2 kg or 3 kg respectively. Only the dimensions in the Z axis change (227 mm for doubles and 340.5 mm for triples). X and Y dimensions remain the same.

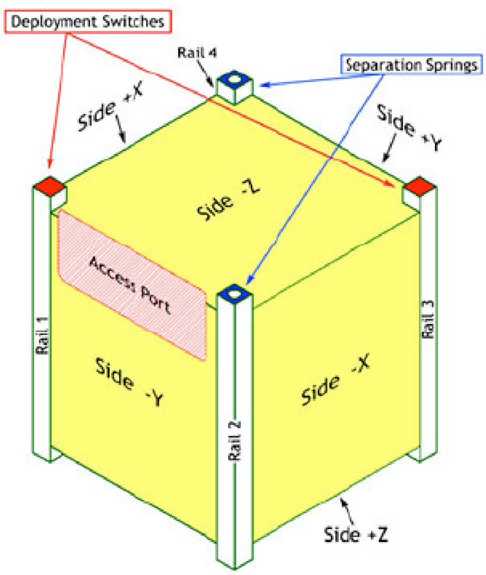

Figure 0.1: CubeSat Isometric Drawing

Structural Requirements

The structure of the CubeSat must be strong enough to survive maximum loading defined in the testing requirements and cumulative loading of all required tests and launch. The CubeSat structure must be compatible with the P-POD.

- Rails must be smooth and edges must be rounded to a minimum radius of 1 mm.
- At least 75% (85.125 mm of a possible 113.5mm) of the rail must be in contact with the P-POD rails. 25% of the rails may be recessed and no part of the rails may exceed the specification.
- All rails must be hard anodized to prevent cold-welding, reduce wear, and provide electrical isolation between the CubeSats and the P-POD.
- Separation springs must be included at designated contact points. Spring plungers are recommended. A custom separation system may be used, but must be approved by Cal Poly launch personnel.
- The use of Aluminum 7075 or 6061-T6 is suggested for the main structure. If other materials are used, the thermal expansion must be similar to that of Aluminum 7075-T73 (P-POD material) and approved by Cal Poly launch personnel.
- Deployables must be constrained by the CubeSat. The P-POD rails and walls are not to be used to constrain deployables.

Electrical Requirements

Electronic systems must be designed with the following safety features.

- No electronics may be active during launch to prevent any electrical or RF interference with the launch vehicle and primary payloads. CubeSats with rechargeable batteries must be fully deactivated during launch or launch with discharged batteries.
- One deployment switch is required (two are recommended) for each CubeSat. The deployment switch should be located at designated points.
- Developers who wish to perform testing and battery charging after integration must provide GSE that connects to the CubeSat through designated data ports.
- A RBF pin is required to deactivate the CubeSats during integration outside the P-POD. The pin will be removed once the CubeSats are placed inside the P-POD. RBF pins must fit within the designated data ports. RBF pins should not protrude more than 6.5 mm from the rails when fully inserted.

Operational Requirements

CubeSats must meet certain requirements pertaining to integration and operation to meet legal obligations and ensure safety of other CubeSats.

- CubeSats with rechargeable batteries must have the capability to receive a transmitter shutdown command, as per FCC regulation.
- To allow adequate separation of CubeSats, antennas may be deployed 15 minutes after ejection from the P-POD (as detected by CubeSat deployment switches). Larger deployables such as booms and solar panels may be deployed 30 minutes after ejection from the P-POD.
- CubeSats may enter LPTM 15 minutes after ejection from the P-POD. LPTM is defined as short, periodic beacons from the CubeSat. CubeSats may activate all primary transmitters, or enter HPTM 30 minutes after ejection from the P-POD.
- Operators must obtain and provide documentation of proper licenses for use of frequencies. For amateur frequency use, this requires proof of frequency coordination by the IARU.
- Developers must obtain and provide documentation of approval of an orbital debris mitigation plan from the FCC.
- Cal Poly will conduct a minimum of one fit check in which developer hardware will be inspected and integrated into the P-POD. A final fit check will be conducted prior to launch. The CAC will be used to verify compliance of the specification. Additionally, periodic teleconferences, videoconferences, and progress reports may be required.

Testing Requirements

Testing must be performed to meet all launch provider requirements as well as any additional testing requirements deemed necessary to ensure the safety of the CubeSats and the P-POD. All flight hardware will undergo qualification and acceptance testing.

The P-PODs will be tested in a similar fashion to ensure the safety and workmanship before integration with CubeSats. At the very minimum, all CubeSats will undergo the following tests.

- Random vibration testing at a level higher than the published launch vehicle envelope outlined in the MTP.
- Thermal vacuum bakeout to ensure proper outgassing of components. The test cycle and duration will be outlined in the MTP.
- Visual inspection of the CubeSat and measurement of critical areas as per the CAC.

Qualification

All CubeSats must survive qualification testing as outlined in the MTP for their specific launch. The MTP can be found on the CubeSat website. Qualification testing will be performed at above launch levels at developer facilities. In some circumstances, Cal Poly can assist developers in finding testing facilities or provide testing for the developers. A fee may be associated with any tests performed by Cal Poly. CubeSats must not be disassembled or modified after qualification testing. Additional testing will be required if modifications or changes are made to the CubeSats after qualification.

Acceptance

After delivery and integration of the CubeSats, additional testing will be performed with the integrated system. This test assures proper integration of the CubeSats into the P-POD. Additionally, any unknown, harmful interactions between CubeSats may be discovered during acceptance testing. Cal Poly will coordinate and perform acceptance testing. No additional cost is associated with acceptance testing. After acceptance testing, developers may perform diagnostics through the designated P-POD diagnostic ports, and visual inspection of the system will be performed by Cal Poly launch personnel. The P-PODs will not be deintegrated at this point. If a CubeSat failure is discovered, a decision to deintegrate the P-POD will be made by the developers in that P-POD and Cal Poly based on safety concerns. The developer is responsible for any additional testing required due to corrective modifications to deintegrated CubeSats.

Appendix B: Link Budget System

Based on the AMSAT Standard Link Budget System [Kin04], the formulas for the link budget were programmed in MS Excel. Antenna, orbit and satellite parameters (especially for the descipted CubSat Mission) were added.

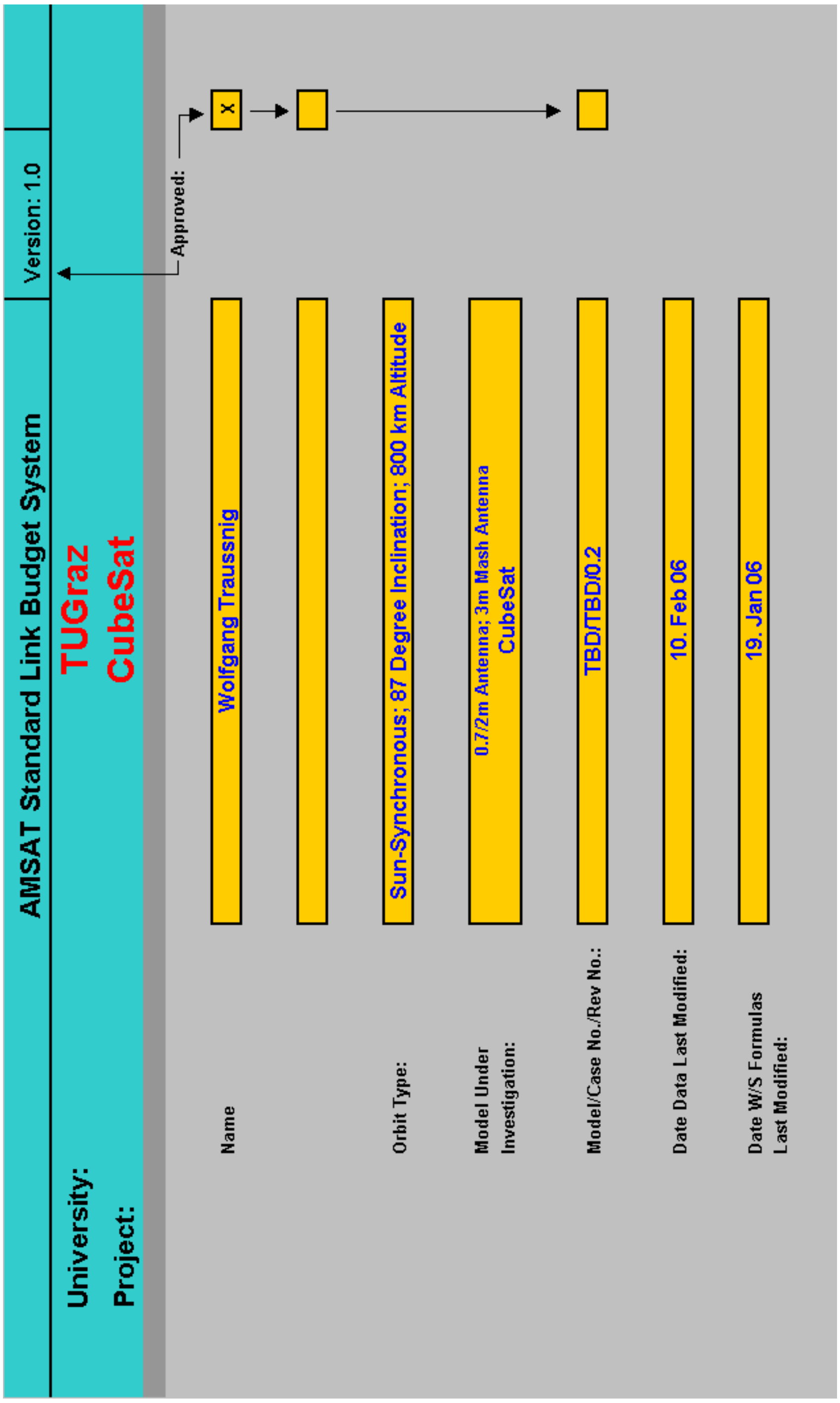

Figure 0.1: Link Budget System

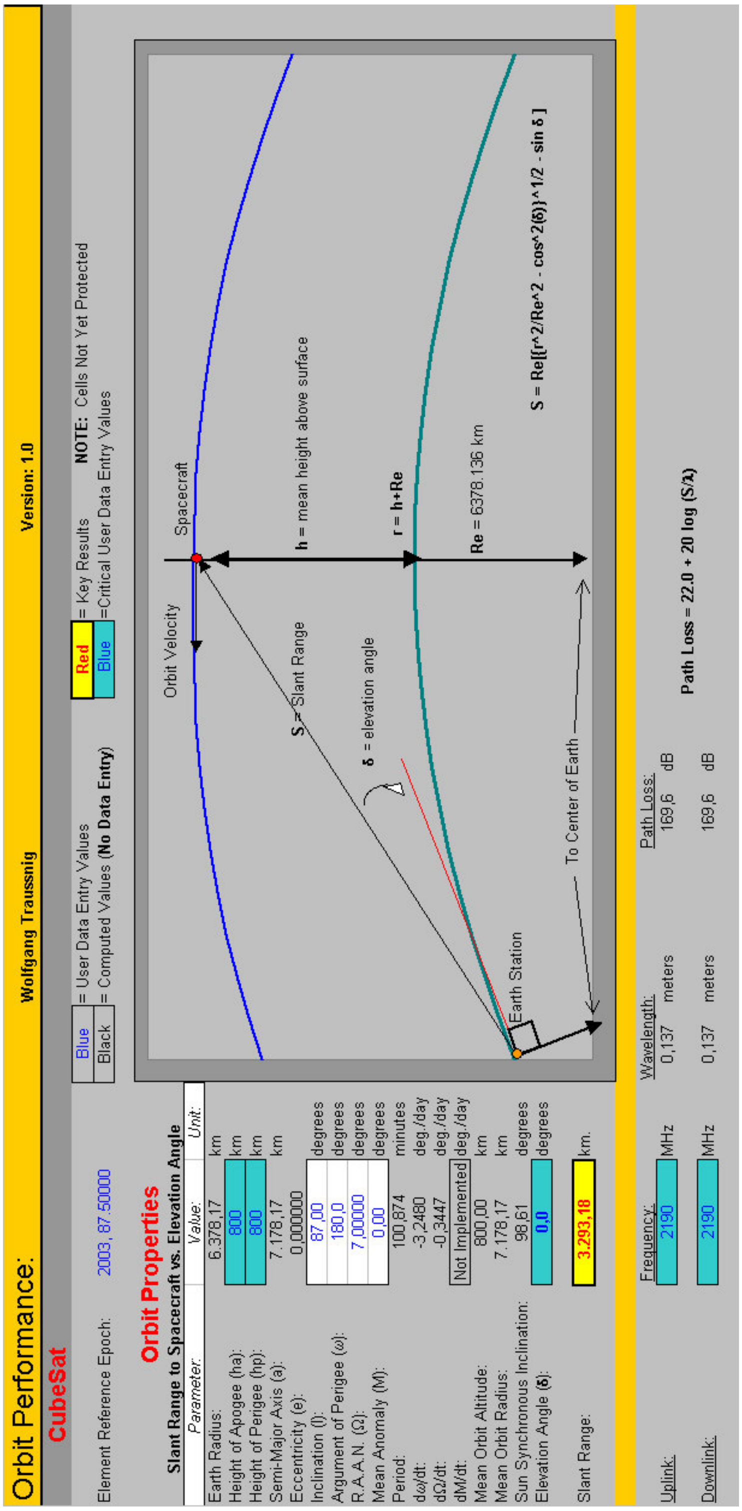

Figure 0.2: Orbit Performance for δ=0 degrees

CubeSat **Downlink Telemetry Budget:**			**Wolfgang Traussnig** **Version: 1.0**	**Date Data Last Modified:**		
Parameter:	*Value:*	*Units:*	*Comments:*			
Spacecraft:						
Spacecraft Transmitter Power Output:	0,5	watts				
In dBW:	-3,0	dBW				
In dBm:	27,0	dBm				
Spacecraft Transmission Line Losses:	0,0	dB				
S/C Connector, Filter or In-Line Switch Losses:	0,0	dB				
Spacecraft Antenna Gain:	0,0	dBiC				
Spacecraft EIRP:	-3,0	dBW	Spacecraft Effective Isotropic Radiated Power (EIRP) [EIRP=Pt x Ltl x Ga]			
Downlink Path:						
Spacecraft Antenna Pointing Loss:	0,0	dB				
Antenna Polarization Loss:	0,0	dB				
Path Loss:	-169,6	dB				
Atmospheric Loss:	0	dB	Use Value Appropriate for Elevation Angle Selected in Orbit Performance W/S.			
Ionospheric Loss:	0,0	dB				
Rain Loss:	0,0	dB				
Isotropic Signal Level at Ground Station:	-172,6	dBW				
Ground Station:				*Ground Station Alternative Signal Analysis Method (SNR Computati*		
------- Eb/No Method -------				***---------- SNR Method -----------***		
Ground Station Antenna Pointing Loss:	0,0	dB		Ground Station Antenna Pointing Loss:	0,0	dB
Ground Station Antenna Gain:	21,1	dBiC		Ground Station Antenna Gain:	21,1	dBiC
Ground Station Transmission Line Losses:	0	dB		Ground Station Transmission Line Losses:	0	dB
Ground Station LNA Noise Temperature:	160	K		Ground Station LNA Noise Temperature:	160	K
Ground Station Transmission Line Temp.:	290	K		Ground Station Transmission Line Temp.:	290	K
Ground Station Sky Temperature:	450	K		Ground Station Sky Temperature:	450	K
G.S. Transmission Line Coefficient:	1,0000			G.S. Transmission Line Coefficient:	1,0000	
Ground Station Effective Noise Temperature:	610	K		Ground Station Effective Noise Temperature:	610	K
Ground Station Figure of Merrit (G/T):	-0,9	dB/K		Ground Station Figure of Merrit (G/T):	-0,9	dB/K
G.S. Signal-to-Noise Power Density (S/No):	55,0	dBHz	Boltzman's Constant: -228,6 dBW/K/Hz	Signal Power at Ground Station LNA Input:	-151,5	dBW
System Desired Data Rate:	9600	bps		Ground Station Receiver Bandwidth:	4.500	Hz
In dBHz:	39,8	dBHz		G.S. Receiver Noise Power (Pn = kTB)	-164,2	dBW
Telemetry System Eb/No:	15,2	dB	Assumes Spectral Efficiency of 1.0 b.p.s./Hz of Bandwidth	Signal-to-Noise Power Ratio at G.S. Rcvr:	12,7	dB
Telemetry System Required Bit Error Rate:	0,00E+00		Assume G3RUH FSK; No Coding; 1 dB Implementation Loss	System Desired Data Rate:	9600	bps
Telemetry System Required Eb/No:	0	dB	This Eb/No Required to meet B.E.R.		39,8	dBHz
System Link Margin:	15,2	dB		Telemetry System Required SNR:	0	dB
				System Link Margin:	12,7	dB

Figure 0.3: Downlink Budget

Parameter:	Value:	Units:	Comments:			
Ground Station:						
Transmitter Power Output:	100,0	watts				
In dBW:	20,0	dBW				
In dBm:	50,0	dBm				
Transmission Line Losses:	0,0	dB				
Connector, Filter or In-Line Switch Losses:	0,0	dB				
Antenna Gain:	21,1	dBiC				
Ground Station EIRP:	41,1	dBW	Ground Station Effective Isotropic Radiated Power (EIRP) [EIRP=Pt x Ltl x Ga]			
Uplink Path:						
Ground Station Antenna Pointing Loss:	0,0	dB				
Antenna Polarization Losses:	0,0	dB				
Path Loss:	-169,6	dB				
Atmospheric Losses:	0,0	dB	Use Value Appropriate for Elevation Angle Selected in Orbit Performance W/S.			
Ionospheric Losses:	0,0	dB				
Rain Losses:	0,0	dB				
Isotropic Signal Level at Ground Station:	-128,5	dBW				
Spacecraft:				*Spacecraft Alternative Signal Analysis Method (SNR Computation):*		
------- Eb/No Method -------				***---------- SNR Method ------------***		
Spacecraft Antenna Pointing Loss:	0,0	dB		Spacecraft Antenna Pointing Loss:	0,0	dB
Spacecraft Antenna Gain:	0,0	dBiC		Spacecraft Antenna Gain:	0,0	dBiC
Spacecraft Transmission Line Losses:	0,0	dB		Spacecraft Transmission Line Losses:	0	dB
Spacecraft LNA Noise Temperature:	513	K		Spacecraft LNA Noise Temperature:	513	K
Spacecraft Transmission Line Temp.:	270	K		Spacecraft Transmission Line Temp.:	270	K
Spacecraft Sky Temperature:	290	K		Spacecraft Sky Temperature:	290	K
S/C Transmission Line Coefficient:	1,0000			S/C Transmission Line Coefficient:	1,0000	
Spacecraft Effective Noise Temperature:	803	K		Spacecraft Effective Noise Temperature:	803	K
Spacecraft Figure of Merrit (G/T):	-27,0	dB/K		Spacecraft Figure of Merrit (G/T):	-27,0	dB/K
S/C Signal-to-Noise Power Density (S/No):	73,1	dBHz	Boltzman's Constant: -228,6 dBW/K/Hz	Signal Power at Spacecraft LNA Input:	-128,5	dBW
System Desired Data Rate:	9600	bps		Spacecraft Receiver Bandwidth:	15.000	Hz
In dBHz:	39,8	dBHz		G.S. Receiver Noise Power (Pn = kTB)	-157,8	dBW
Telemetry System Eb/No:	33,3	dB	Assumes Spectral Efficiency of 1.0 b.p.s./Hz of Bandwidth	Signal-to-Noise Power Ratio at S/C Rcvr:	29,3	dB
Telemetry System Required Bit Error Rate:	0,00E+00		Assume Non-Coherent FSK; No Coding; 1 dB Implementation Loss	System Desired Data Rate:	9600	bps
Telemetry System Required Eb/No:	0,0	dB	This Eb/No Required to meet B.E.R.		39,8	dBHz
System Link Margin:	33,3	dB		Telemetry System Required SNR:	0,0	dB
				System Link Margin:	29,3	dB

Figure 0.4: Uplink Budget

References

[AAA97] American Institute of Aeronautics and Astronautics, *Moving Mechanical Assemblies for Space and Launch Vehicles,* AIAA Standard, S-114-2005, 2005.

[ABV+04] L. Alminde, M. Bisgaad, D. Vinter, T. Viscor, and K. Z. Østergard. *The AAU-CubeSat student satellite project : architectural overview and lessons learned"* in Proceedings of the 16th IFAC Symposium on Automatic Control in Aerospace, 2004.

[Ams] AMSAT. http://www.amsat.org

[BMB88] S Basu, E Mackenzie, and S Basu. *Ionospheric Constraints on VHF/UHF Communications Links during Solar Maximum and Minimum Periods*, *Radio Science*, vol. 23, pp. 363-372,1988.

[BJ94] K. Baker and D. Jansson. *Space satellites from the world's garage - the story of AMSAT*," presented at the National Aerospace and Electronics Conference, Dayton, Ohio, May 1994.

[BNT97] Williams Beech, Douglas Nielsen, and Jack Taylor, *AX.25 Link Access Protocol for Amateur Packet Radio,* Tuscon Amateur Radio Corporation, 1997.

[Ccs] Consultative Committee for Space Data Systems. http://www.ccsds.org

[Cha01] Jeremy Chan. *GPS BOARD AND ANTENNA SPECIFICATIONS,* V 1.1, March 14, 2001

[Cla05] Emily Clarke. *Using Amateur Satellites*, Presentation, 2005.

[Cle04] Michel Clénet. *Design of a UHF Circularly Polarized Patch Antenna as a feed for a 9.1 metre Parabolic Reflector,* TECHNICAL MEMORANDUM, DRDC Ottawa TM 2004-139, June 2004.

[Doh00] Doherty, P.. *Ionospheric Scintillation Effects in Equatorial and Auroral Regions*, Salt Lake City, Utah, p. 662-671, ION GPS 2000.

[Ea4] EA4TX. http://www.ea4tx.com/

[Eit02] EiT. Proposals for the communication subsystem onboard NCUBE, spring 2002, (http://www.rocketrange.no/ncube/documents/NCUBE-rapport-COM.pdf).

[Eme95] Emerson, D., AA7FV, *The Gain of the Axial- Mode Helix Antenna,* Antenna Compendium Volume 4, ARRL, pp.64-68, 1995.

[FHR00] Wanxuan Fu, Shaowei Han and Chris Rizos. *Real-Time Ionospheric Scintillation Monitoring*, The University of New South Wales, Australia, 2000.

[Fwm] Fort Wayne Metalls. http://www.fwmetals.com

[Itu04] INTERNATIONAL TELECOMMUNICATION UNION (ITU), *Radio Regulations Edition of 2004*, No. 119-04-Rev-04, Geneva, 29 November 2004.

[Ion] Ionosphere – Wikipedia. http://en.wikipedia.org/wiki/Ionosphere

[Kin04] Jan A. King. *AMSAT/IARU Satandard Link Budget System*, Cal Poly State University, 2004.

[KF88] M. Knight, and A. Finn. *The Effect of Ionospheric Scintillation on GPS*, *ION GPS*, Nashville, TN, 1998.

[Kou03] O. Koudelka, *Satellite Communications,* Folien zur Vorlesung Nachrichtensatelliten, Institut für Nachrichtentechnik, Graz, 1993.

[Kra77] JD. Kraus. *A 50-Ohm Impedance for Helical Beam Antennas,* IEEE Transactions on Antennas and Propagation, p.913, November 1977.

[Kra95] JD. Kraus. (W8JK), *A Helical-Beam Antenna Without a Ground Plane,* IEEE Antennas and Propagation Magazine, p.45, April 1995.

[Lct05] L3 Communications Telemetrie West. *Miniature S-Band T&C Transceiver MSX-765,* Rev. A, 2005.

[LKW+02] B. Larsen, D. M. Klumpar, M. Wood, G. Hunyadi, S. Jepsen, M. Obland, *Microcontroller Design for the Montana EaRth Orbiting Pico-Explorer (MEROPE) CubeSat-Class Satellite*, 2002 IEEE Aerospace Applications Conference Proceedings, March 9-16, 2002.

[LLR+02] M. Long, A. Lorenz, G. Rodgers, E. Tapio, G. Tran, K. Jackson, R. Twiggs, and T. Bleier. *A CubeSat derived design for a unique academic research mission in earthquake signature detection*, presented at 16th Annual AIAA/USU Conference on Small Satellites, Logan, Utah, 2002.

[MHJ01] Terence H. McLoughlin, Justin Maloney-Hahn and Juan F. Jimenez. *CubeSat System Specification Document*, 2001.

[Ott02a] Jan Otterstad. *Antenna system for NCUBE,* Norgens Teknisk-Naturvitenskapelige Universitet, September 2002.

[Ott02b] Jan Otterstad. *Design Document for the Antenna Subsystem,* Version 1, 2002.

[Owe00] Michael R. Owen, *Nova for Windows*, Northern Lights Software Associates, draft 10, 4-2-00.

[Pol05] Mario Polaschegg. *Study of a Cube-Sat Mission*, Master Thesis, Karl-Franzens University of Graz, Graz, Austria, 2005.

[RVT01] I. Rutter, T. Vladimirova, H. Tiggeler, *A CCSDS Software System for a Single-Chip On-Board Computer of a Small Satellite,* AIAA Small Satellites Conference, SSC01-VI-4, 2001.

[San04] Raj Sanjai, *Radiocommunications Regulations* (General User Radio Licence for Visiting Amateur Radio Operators) Notice 2004, New Zealand Gazette Notice: go4382, 2004.

[Sim93] K. Simonyi, *Theoretische Elektrotechnik,* 10. Auflage, ISBN 3-335-00375-6, 1993.

[SKJ01] S Skone, K Kundsen, and M de Jong. *Limitation in GPS Receiver Tracking Performance under Ionospheric Scintillation Conditions*, Physics and Chemistry of Earth (A), vol. 26 pp. 613-621, 2001.

[Sko02] S. H. Skone. *GPS Receiver Tracking Performance under Ionosheric Scintillation Conditions,* Department of Geomatics Engineering, University of Calgary.

[Smt] Sandvik Materials Technology. http://www.smt.sandvik.com

[Ssc05] Surrey Space Centre, University of Surrey. *Small satellites home page*, April 2005, http://centaur.sstl.co.uk/SSHP/index.html

[Stu98] W.L. Stutzman; *Antenna theory and design*, 2nd ed. 1998.

[Tew05] S.K Tewksbury, *Basics of the Dipole Antenna,* Dept. of Electrical and Computer Engineering Stevens Institute of Technology Hoboken, NJ, 1991.

[Tor05] Armen Torrian. *CubeSat Design Specification*, Updated Specification, Revision 9, 2005.

[Tug] TUGSAT-1. http://www.tugsat.tugraz.at/home

[WHC05] S. Waydo, D. Henry, and M. Campbell. *CubeSat design for LEO-based Earth science missions*, April 2005, http://www.cds.caltech.edu/~waydo/papers/IEEE2002.pdf